Assessment of mercury and organic matter in thermokarst affected lakes of the Mackenzie Delta uplands, NT, Canada

Ramin Deison

Thesis submitted to the

Faculty of Graduate and Postdoctoral Studies

University of Ottawa

in partial fulfillment of the requirements for the

M.Sc. degree in the

Ottawa-Carleton Institute of Biology

Thèse soumise à la

Faculté des études supérieures et postdoctorales

Université d'Ottawa

en vue de l'obtention de la maîtrise ès sciences

L'Institut de biologie d'Ottawa-Carleton

Table of Contents

Abstract

The Mackenzie Delta region of the Northwest Territories, Canada, has experienced rapid climate warming in the past century resulting in rapidly thawing permafrost in this region. This thesis examines spatial and temporal changes to sediment organic carbon and mercury flux in lakes from thermokarst regions by comparing sediment cores from lakes with and without retrogressive thaw slumps on their shorelines. We show that sediments from lakes with permafrost thaw slump development on their shorelines (slump lakes) had higher sedimentation rates as well as lower total Hg, methyl mercury (MeHg), and labile OC fractions when compared to lakes where thaw slumps were absent. Total Hg and MeHg concentrations in sediments were correlated with total organic carbon (TOC), S2 (labile algal-derived OC), and inferred chlorophyll *a* content, indicating an association between autochthonous organic carbon and Hg in these sediments. Correlations between mercury and S2 in these study lakes generally support the hypothesis that algal-derived materials correlate with Hg concentration in sediments. We observed higher S2 concentrations in reference lakes than in slump lakes, likely due to uninterrupted algal production, lower dilution by flux of inorganic matter, and possibly better anoxic preservation in reference lakes compared to slump lakes. It is evident that thaw slump development in this thermokarst region increases inorganic sedimentation in lakes, while decreasing concentrations of organic carbon and associated Hg and MeHg in sediments.

Résumé

La région du Delta du Mackenzie, dans les Territoires du Nord-Ouest au Canada, a subit, ce siècle dernier, des changements climatiques rapides qui ont mené au dégel précipité du pergélisol dans cette région. Cette thèse examine les changements spatiaux et temporels du carbone organique et du flux du mercure dans les sédiments de lacs des régions thermo karstiques en comparant des carottes de sédiment de lacs avec et sans glissement du sol provoqué par le dégel sur leur littoral. Nous démontrons que les lacs avec un glissement du sol en développement sur leur littoral (lac perturbé) possèdent un taux de sédimentation plus élevé, de même que des concentrations en Hg, en méthyle mercure (MeHg) et des fractions de carbone organique (OC) labile plus faibles que les lacs sans glissement du sol. Les concentrations totales de Hg et de MeHg dans les sédiments sont corrélées avec le carbone organique total (TOC), le S2 (OC labile dérivé des algues) et le contenu de chlorophylle *a* inféré; indiquant un lien entre le carbone organique autochtone et le Hg dans ces sédiments. Les corrélations entre le mercure et le S2 dans ces lacs étudiés supportent généralement l'hypothèse que les matériaux dérivés des algues sont en corrélation avec la concentration en mercure dans les sédiments. Nous pouvons observer des concentrations en S2 plus importantes dans les lacs de référence en comparaison avec les lacs perturbés. Ceci est probablement dû à une production algale non interrompue, une dilution plus faible causée par le flux de la matière inorganique et possiblement une meilleure préservation anoxique observables dans les lacs de référence. Il est évident que le développement de glissement du sol dans cette région thermokarstique augmente la sédimentation inorganique dans les lacs tout en diminuant leur concentration en carbone organique ainsi qu'en Hg et en MeHg dans les sédiments.

Acknowledgments

First and foremost I would like to thank my supervisor Dr. Jules Blais for his tremendous help, valuable advice and professional, scientific and financial support. I am also very grateful to Linda Kimpe, and Dr. Emmanuel Yumvihoze who provided advice, guidance and support. I would also like to thank the co-authors of the included articles for their valuable comments and suggestions which greatly improved the manuscripts.

This study was funded by a Natural Sciences and Engineering Research Council (Canada) Strategic Projects grant to JMB, JPS, and MP. Logistical support was provided by the Polar Continental Shelf Program (PCSP). We thank Peter deMontigny for field assistance.

Many thanks to other graduate students Adam Houben, Jamie Doyle, and Ahmed Al-Ansari for all their help. I also wish to thank my very dear friend Alexis Gagnon for being extremely supportive and kind. I am very glad for knowing such a great friend through my education.

My special thanks to my parents, Monavar and Abdal who raised me, taught me, and guided me without whose support none of this would have been possible.

Last but not least, thanks so much to my wife Mitra, for her patience, support, understanding and encouragement which makes my life joyful.

I would like to dedicate this thesis to my dear parents and my wife!

1.0-Introduction

Permafrost degradation is already changing the polar landscape with a significant increasing trend which might accelerate in coming decades. Currently, about one fifth of the exposed surface of the Earth is underlain by some form of permafrost, including 22% of the land area in the Northern Hemisphere (Davis 2001). Permafrost covers an area of 26 million km^2 globally (ACIA, 2005), 50% of Canada, and 85% of Alaska (Ming-Ko*et al.*, 1992; Jorgenson & Osterkamp, 2005).

Northwestern Canada, including the Mackenzie Delta region, has experienced some of the world's most pronounced warming during the past 50 years (ACIA, 2005). Temperature monitoring at Inuvik since the 1960s has recorded an increase in mean annual temperature of 2.3ºC (Dyke 2000) and an increase of up to 8^oC in the Canadian Arctic is predicted by 2100 (IPCC, 2007). This makes the Mackenzie Delta region one of the most thaw- sensitive permafrost regions in Canada (Lantz and Kokelj, 2008), and is where recent increases in permafrost temperatures have been recorded (Smith et al., 2005; Kokelj et al. 2007). Such increasing permafrost temperatures have been due to atmospheric warming, resulting in an increased frequency of terrain disturbances due to the thawing and settling of ice rich terrain (Jorgenson *et al.*, 2006) which can significantly affect local water quality, even if they only occupy 2% of a lake's catchment area (Kokelj*et al.*, 2005).

Recent studies predict that the influx of permafrost thawing material into freshwater systems will introduce a variety of materials that were previously trapped in the frozen ice and soil (Kokelj and Burn, 2005; Kokelj et al., 2005), which is likely to change the amount of

metallic and organic contaminants entering freshwater lakes, but there is still a significant gap in our knowledge of how ecosystems will respond to climate warming in thermokarst regions.

Studies of mercury from hydroelectric reservoirs have shown that rapid decomposition and oxygen depletion in soils results in increased mercury and methyl mercury release to surface waters (St-Louis et al. 2004, Brigham et al. 2002), though comparable information for permafrost has not been collected. Mercury contamination has been observed in remote areas such as the Arctic, and as such, it has become known as a global pollutant (Ariya et al., 2004). It is estimated that 60% of atmospheric mercury is deposited on land and 40% on water and in the Arctic. Most of the land deposited mercury is likely to enter aquatic environments through melt-water and runoff (Macdonald et al., 2005). Likewise, previous studies on contaminated soils showed that continuous permafrost typically acts as an effective barrier preventing contaminants from infiltrating into the ground (e.g. Braddock and McCarthy 1996), and some (e.g., Curtosi et al. 2007) have predicted that thawing permafrost will release contaminants to surface waters with unknown ecological consequences. Meanwhile, some studies have discussed recent increases in algal productivity from pronounced climate warming in Arctic lakes as a possible factor for increasing contaminant delivery to lake sediments (Macdonald et al. 2005; Stern et al. 2005, 2009; Outridge et al. 2007; Carrie et al. 2010; Sanei et al. 2010). Also Outridge et al. (2007) demonstrated how autochthonous organic flux to sediments (as determined by the S2 fraction) explained between 87-91% of the variance in total Hg flux to two High Arctic lakes and suggested that S2 or algal-derived carbon was primarily responsible for mercury scavenging in the water column and this effect is likely on the rise in recent decades due to climate-related increases in algal productivity due to climate warming especially during the past several decades.

However, another recent multi-site comparative analysis by Kirk et al. (2011a) showed that algal scavenging does not always explain Hg deposition to sediments adequately, based on a broad survey of lake sediment cores across the Canadian Arctic. This hypothesis has been particularly contentious (Outridge et al. 2011, Kirk et al, 2011b) because it holds direct industrial emission responsible for only a fraction (less than 40%) of increased mercury in the 20th century in sediment archives (Outridge et al. 2007; Stern et al. 2009). Despite the controversy, this algal scavenging hypothesis may offer one explanation for mercury increases in some Arctic lake sediment archives despite decreasing atmospheric mercury concentrations (Fain et al. 2009; Li et al. 2009).

In the present study we used a paired, comparative analysis where retrogressive thaw slumps werepresent and absent. We examined sediments from 14 and 8 lakes for our spatial and temporal analyses respectively in the Mackenzie Delta uplands, NWT, to determine how retrogressive thaw slump development from degrading permafrost affected the delivery of mercury (Hg),methylmercury (MeHg) and organic carbon (OC) to lake sediments in thermokarst regions.We predicted that sediment cores from lakes disturbed by thawing permafrost would have higher inorganic sedimentation rates, lower total Hg concentration, and lower total organic carbon and S2 organic carbon content than reference lakes where thaw slumps were absent. We investigated whether the history of permafrost thaw slump development could be reconstructed from lake sediment cores. We also predicted that, within each sediment profile, Hg would correlate with S2 carbon as predicted by the algal scavenging hypothesis.

2.0-Spatial assessment of mercury and organic matter in thermokarst affected lakes of the Mackenzie Delta uplands, NT, Canada

Ramin Deison[1*], John P. Smol[2], Steve Kokelj[3], Michael F.J. Pisaric[4], Alex Poulain[1], Hamed Sanei[5], Josh Thienpont[2], Jules M. Blais[1]

[1]Program for Chemical and Environmental Toxicology, Department of Biology, University of Ottawa.

[2]Paleoecological Environmental Assessment and Research Lab (PEARL), Department of Biology, Queen's University, Kingston.

[3]Water Resources Division, Indian and Northern Affairs Canada, Yellowknife.

[4]Department of Geography and Environmental Studies, Carleton University, Ottawa.

[5]Geological Survey of Canada-Calgary.

2.1-Abstract

Using a paired, comparative analysis, we examined sediments from 14 thermokarst affected lakes in the Mackenzie Delta uplands, NWT, to determine how retrogressive thaw slump development from degrading permafrost affected the delivery of mercury (Hg) and organic carbon (OC) to lakes. We show that sediments from the lakes with permafrost thaw slump development on their shorelines (slump lakes) had higher sedimentation rates and lower total Hg, methyl mercury (MeHg), and labile OC fractions compared to lakes where thaw slumps were absent. Total Hg and MeHg concentrations were correlated with total organic carbon (TOC), S2 (labile algal-derived OC), and sediment inferred chlorophyll *a* content, indicating an association between autochthonous organic carbon and Hg in these sediments. Spatial and temporal correlations between mercury and S2 in all our study lakes except one pair (2a and 2b) generally supports the hypothesis that algal-derived materials may be sources of Hg to sediments. We observed higher S2 and particulate organic carbon (POC) concentrations in reference lakes than in slump lakes, likely due to uninterrupted algal production, lower dilution by flux of inorganic siliciclastic matter, and possibly better anoxic preservation in reference lakes compared to slump lakes. It is evident that thaw slump development in this thermokarst region increases inorganic sedimentation in lakes, while decreasing concentrations of organic carbon and associated Hg and MeHg in sediments.

2.2-Introduction

Thawing permafrost is already changing the polar landscape and will likely accelerate in coming decades. Consequent to thaw, significant changes in hydrology, organic carbon pathways and freshwater resources are also expected (ACIA 2005). Currently, about one fifth of the exposed surface of the Earth is underlain by some form of permafrost, including 22% of the land area in the Northern Hemisphere (Davis 2001). Since the 1970s there has been a steady increase in permafrost temperatures in many Arctic regions including Alaska (Lachenbruch and Marshall 1986, Jorgenson et al. 2006), western Canada (Burn 2002) and Siberia (Pavlov 1994), although rates of permafrost thaw have been slower in some parts of eastern Canada (Serreze et al. 2000).

Recent studies predict that the influx of retrogressive thaw slump material into freshwater systems will introduce a variety of materials that were previously trapped in the frozen ice and soil (Kokelj and Burn, 2005; Kokelj et al., 2005). As the active layer deepens and more unfrozen flow pathways develop in the permafrost, increased geochemical weathering from drainages is expected (Hobbie et al. 1999, Kokelj et al. 2005, Prowse et al. 2006), leading to changes in freshwater chemistry, including increases in concentrations of ions such as Na^{+}, K^{+}, Mg^{+2}, SO_4^{-2}, Cl^{-}, and HCO_3^{-}, and decreases in dissolved organic carbon (DOC) (Kokelj et al. 2005). The extent to which thawing permafrost will change the amount of metallic and organic contaminants entering freshwater lakes is a significant gap in our knowledge of how ecosystems will respond to climate warming in thermokarst regions. We know from studies of mercury from hydroelectric reservoirs that rapid decomposition and oxygen depletion in soils results in increased mercury and methyl mercury release to surface waters (St-Louis et al. 2004, Brigham et al. 2002), though

comparable information for permafrost has not been collected. We also know from some studies on contaminated soils that continuous permafrost typically acts as an effective barrier preventing contaminants from infiltrating into the ground (e.g. Braddock and McCarthy 1996), and some (e.g., Curtosi et al. 2007) have predicted that thawing permafrost will release contaminants to surface waters with unknown ecological consequences. In addition, recent increases in algal productivity from pronounced climate warming in Arctic lakes may also increase contaminant delivery to lake sediments (Macdonald et al. 2005; Stern et al. 2005, 2009; Outridge et al. 2007; Carrie et al. 2010;Sanei et al. 2010). Several have suggested that the delivery of mercury to aquatic systems may be strongly influenced by variations in the source, type, and relative quantity of autochthonous versus allochthonous organic matter (Jackson 1986; Kainz et al. 2003; Sanei and Goodarzi, 2006). Likewise, some studies on northern lakes have reported significant associations between temporal trends of mercury and proxies for autochthonous organic matter (Outridge et al. 2007; Carrie et al. 2009; Stern et al. 2009). These studies suggested that algal-derived carbon is primarily responsible for mercury scavenging in the water column and this effect is likely on the rise in recent decades due to climate-related increases in algal productivity. However, a recent multi-site comparative analysis by Kirk et al. (2011a) showed that algal scavenging does not always explain Hg deposition to sediments adequately, based on a broad survey of lake sediment cores across the Canadian Arctic. This hypothesis has been particularly contentious (Outridge et al. 2011, Kirk et al, 2011b) because it holds direct industrial emission responsible for only a fraction (less than 40%) of increased mercury in the 20th century in sediment archives (Outridge et al. 2007; Stern et al. 2009).

Despite the controversy, this algal scavenging hypothesis may offer one explanation for mercury increases in some Arctic lake sediment archives despite decreasing atmospheric mercury concentrations (Fain et al. 2009; Li et al. 2009).

Here we assessed mercury sedimentation in lakes with catchments affected by thawing permafrost in a case-control analysis of lakes where retrogressive thaw slumps are present and absent (Figure2.1). This pairwise comparative study design is intended to provide an early indication of the influence of thawing permafrost on mercury delivery to lake sediments in thermokarst regions.

2.3-Methods

2.3.1-Study Area

We examined sediment cores of fourteen lakes along a transect east of the Mackenzie Delta, from Inuvik to Richards Islands (Figure 2.1). These lakes were chosen following an analysis of aerial photographs and field surveys (Kokelj et al. 2005). Seven study lakes have retrogressive thaw slumps on their shorelines (i.e. degraded permafrost) and the other seven lakes are in undisturbed catchments. The location and characteristics of the study lakes are given in Table 2.1.

2.3.2-Sample Collection and Preparation

Sediment cores measuring 35-40 cm in length were recovered from the centre of the fourteen lakes in summer 2007-2008 using a Glewgravity corer and Plexiglas core tubes (Glew 1989). All the cores were sub-sampled at 0.25 cm intervals between 0 and 15 cm and at 0.5 cm intervals from 15 cm to the bottom with a vertical core extruder (Glew 1988, Glew et al. 2001). The sediment samples were placed into air-tight centrifuge tubes and plastic bags, placed on ice, and transported in a dark cooler to the laboratory the same day. Sediments were then stored in a freezer for future analysis. The sediments were sub-sampled and freeze-dried for 2 to 3 days, and the dried sediments were ground for radiometric analysis, THg, MeHg and Rock-Eval analysis.

2.3.3-^{210}Pb Inventories and Flux calculations

Sediment cores were radiometrically dated using gamma (γ) spectrometry. The fourteen sediment cores were analyzed for the activity of ^{210}Pb, ^{137}Cs and ^{226}Ra. Analysis of ^{210}Pb was performed at 12-15 selected depth intervals in the sediment cores to determine the sediment age, and the sediment accumulation rate (Appleby 2001). Samples were ground and homogenized, then added to centrifuge tubes (8.4 cm high and 1.5 cm outer diameter) to a height of 2 cm. Sediment samples were settled for a minimum of two days before sealing with an epoxy resin. Sealed samples were left to reach secular equilibrium for a minimum of 3 weeks, then counted using a digital high purity germanium well detector (DSPec, Ortec), following methods in Appleby (2001). Samples were counted for 23 hours (82,800 seconds). The resulting spectrum files showed ^{210}Pb activity with a peak at 46.5 keV, and ^{137}Cs at 662 keV. ^{226}Ra activity was determined by γ-ray emissions of its daughter isotope ^{214}Pb, resulting in peaks at 295 and 352

keV. ^{210}Pb and ^{137}Cs counts were performed to date the sediment cores by gamma spectrometry, using a digital high purity germanium well detector (DSPec, Ortec), following methodsin Appleby (2001). Long-term sedimentation rates were determined for each core using the slope of the ln^{210}Pb activity and the cumulative dry mass in the core (Appleby and Oldfield 1978). ^{137}Cs activity (from atmospheric fallout of nuclear weapons, peaking in 1963) was measured to verify ^{210}Pb dates. Focus factors (FF) were determined by dividing the deposition rate of excess ^{210}Pb in each sediment core [excess ^{210}Pb inventory (Bq m^{-2}) x ^{210}Pb decay constant (0.03114 yr^{-1})] by the estimated atmospheric excess ^{210}Pb deposition rate at this latitude (50 Bq m^{-2} yr^{-1}, Omelchenko et al. 1995).

Fluxes such as Hg flux (HgF), anthropogenic Hg fluxes (ΔHgF), enrichment factors (EFs) , as well as Hg fluxes adjusted for sedimentation and an adjusted anthropogenic Hg flux ($\Delta F_{F,adj}$; calculated using the equation of Perry et al., 2005) were calculated as follows:

1) F (µg m^{-2} y^{-1}) = Concentration (µg g^{-1}) x ^{210}Pb-derived sedimentation rates (g m^{-2} y^{-1})

2) ΔF (µg m^{-2} y^{-1}) = F_{recent} (post-1990) - $F_{pre\text{-}ind}$(pre-industrial; pre-1850

3) EF= recent (post-1850)/pre-industrial Hg concentrations

4) $\Delta F_{F,adj} = F_{Frecent} - F_{Fpre\text{-}ind} - (F_{Fpre\text{-}ind}$x sedimentation ratio- $F_{Fpre\text{-}ind})$

2.3.4-THg Analysis and Various Flux Calculations

Homogenized freeze-dried sediment samples were analyzed for total mercury using an automatic mercury analyzer based on thermal decomposition, dual step gold amalgamation and detection via Cold-Vapor Atomic Absorption using a Sp-3D mercury analyzer (Nippon instrument Corp) with detection limit of 0.01ng per sample size. Sample mass ranged between 25-30 mg. The accuracy of our analysis was estimated by running blanks and spikes as well as two reference materials during the analytical procedure. Spikes from a stock of Mercury Reference Solution (certified 1000 μg g^{-1} ± 1 %; Fisher Scientific CSM114-100) were brought to a concentration of 50 ng g^{-1} and were tested every 5 samples. The average recovery of the spikes was 102 % ± 5(SD), (n = 12). According to procedural blanks, no contamination was observed during THg analysis. Reference Materials were tested every 4-5 samples and average percentage recovery for MESS-3 (Marine Sediment Certified Reference Materials from NRC with concentration of 91 ± 9 ng g^{-1} was 96 % ± 4 (SD), (n = 35).

2.3.5-MeHg Analysis

Methylmercury concentration in the homogenized freeze-dried sample sediments were determined by capillary gas chromatography coupled with atomic fluorescence spectrometry (GC-AFS) as described by Cai et al. (1997), with a detection limit of 0.02 ng per sample size. Sample mass ranged between 0.4 and 1 g.

Freeze-dried sediments consisting of 0.4 to 1.0 g were weighed into a 50-mg polypropylene centrifuge tube 5ml of acidic KBr-$CuSO_4$ (3:1) mixture was added and, after vigorous mixing (with vortex), 5 ml of CH_2Cl_2 was added quantitatively. The tube was tightly

capped and left to react for 1 h in the dark, followed by 2 h of vigorous mixing with a shaker (330 rpm). The sample was centrifuged at 5,000 rpm for 15 min to break the emulsion that may have formed. An exact known amount (by weight) of the extract was transferred to clean 7-ml glass vials, then samples were subjected to sodium thiosulfate clean-up and the organomercury species were isolated as their bromide derivatives and subsequent extraction into a small volume of dichloromethane followed by GC-AFS analysis.

Accuracy was ensured in sediment analysis by procedural blanks and spiked samples. The average recovery of spiked samples was 97.5 % ± 5 (SD), (n = 12) and analysis of procedural blanks revealed no contamination during MeHg analysis. The average recovery of Reference Material IAEA-405 (Trace and Major Elements in Estuarine Sediments from IAEA, Monaco with concentration of 5.49 ng g^{-1}) was 96 % ± 4 (SD), (n = 8).

2.3.6-Organic Geochemistry (Rock-Eval Analyses)

We applied Rock-Eval® 6, (Vinci Technologies, France) for the quantitative and qualitative study of OM in the recent sediments. The Rock-Eval® 6 method consists of pyrolysis (under inert conditions) and then oxidation , both performing a temperature programmed heating of the sediments (30-50 mg) at a rate of 25°C per minute.

The analytical method involves placing the dried sediment sample into a pyrolysis chamber under inert, oxygen-free atmosphere (either helium or nitrogen) and heating it from 300-650°C. S1 and S2 are analyzed by flame-ionization detection (FID) and measured as mgHC/g (HC = hydrocarbons). S3 is measured by infrared (IR) detection, and determines CO_2 and CO emitted from the sample, and is measured as mg CO_2/g (or mg CO/g). Rock Eval 6

analysis also provides measures of hydrogen index(HI) and Oxygen index (OI) expressed as mg HC g^{-1} TOC and mg CO_2 g^{-1} TOC respectively, which are indicative of kerogen type (La Fargue et al. 1998; Peters et al. 2005).

The S1 fraction consists of volatile, short-chain hydrocarbons, pigments, and some humic substances, and is released due to initial thermal de-volatilization of highly labile and volatile organic compounds including some pigments, organic acids, and bio-lipids and the S2 fraction is released due to thermal cracking of kerogen and consists of higher molecular weight aliphatic hydrocarbons corresponding to the biomolecular structure of algal cell walls (Lafargue et al. 1998, Sanei et al. 2005). The S2 fraction is commonly referred to as the 'algal derived' fraction (Outridge et al. 2007, Stern et al. 2009, Carrie et al. 2010). S3 represents CO_2 produced during pyrolysis and consists of oxygen-containing organic compounds, typically from higher plants and terrestrially-derived organic matter. Because of the difficulty in determining precise sources of S3, it has not been used in sediment studies, and will not be considered here. The pyrolyzable carbon (PC) is equal to the sum of S1, S2 and S3 fractions. The refractory organic carbon (residual carbon; RC) is released only after high temperature (400-850°C) incineration of remaining organic matter in presence of oxygen, immediately following the pyrolysis stage. It is composed mostly of highly resistant OM, such as lignins and cellulosic materials from higher plants, and char. It is measured by infrared (IR) detection. Total organic carbon (TOC) is sum of the PC and RC in a given sample (Lafargue et al., 1998; Behar et al., 2001).

2.3.7-Inferred Chlorophyll a *in Sediments*

Sedimentary chlorophyll *a*content was inferred using visible reflectance spectroscopy (VRS), a method that provides an indication of overall lake production (Michelutti et al. 2005). Samples were freeze dried, sieved (125 µm), and analyzed on a FOSS NIRSystems Model 6500 rapid content analyzer. The portion of the electromagnetic spectrum from 650-700 nm was analyzed in order to detect both chlorophyll *a*and its derivatives (pheophytin*a* and pheophorbide*a*), allowing VRS-chlorophyll *a*to track changes in production over time, and not simply diagenesis (Wolfe et al. 2006, Michelutti et al. 2010).

2.3.8-Statistical Analyses

All data were analyzed usingOrigin Lab 7 software (Origin Lab Corporation MA, USA). Simple linear regressions analysis was used to analyze the relationships between total mercury,S2, inferred chlorophyll *a*, and sedimentation rates. Student t-test was used to test the difference between disturbed and undisturbed lakes with respect to total mercury, S2, inferred chlorophyll *a*and, sedimentation rates.

2.4-Results and Discussion

2.4.1-Sediment Appearance

The sediment lithology was fairly homogenous in our 14 cores, grading from light brown or dark brown to black sediment at the bottom. However, surface sediments from disturbed lakes tended to be greyer in color, likely due to weathering of exposed clays from thaw slumps (Kokelj et al. 2005), and their lower organic content (Figure 2.2).

2.4.2-^{21}PbDating and Sedimentation

Focus-corrected sedimentation rates in disturbed lakes (269±66 SD g m^{-2} yr^{-1}) were more than double those in undisturbed lakes (120±37 g m^{-2} yr^{-1}) indicating higher incoming material to lakes disturbed by retrogressive thaw slumps. Higher sedimentation rates in disturbed lakes might be due to climate-induced changes to permafrost degradation as a result of an increase in mean annual temperature of 2.3ºC in the study region since the 1960s (Dyke 2000, Lantz and Kokelj 2008) and extensive warming in the Mackenzie Delta since the late 19th and early 20th centuries (Pisaric et al. 2007).

Inorganic sedimentation rates largely accounted for differences in sedimentation rates, with 253 ± 65 SD g m^{-2} y^{-1} in disturbed lakes compared to 104 ± 34 SD g m^{-2} y^{-1} ($t_{(2),12}$ = 5.32, p<0.001). The focus-corrected total organic carbon sedimentation rates were similar between disturbed lakes (16.3 ± 9.4 SD g m^{-2} y^{-1}) and undisturbed lakes (15.6 ± 6.8 SD g m^{-2} y^{-1}, $t_{(2),12}$ = 1.78, p = 0.85), indicating fairly uniform organic sedimentation rates regardless of whether they were disturbed by retrogressive thaw slumps or not. Likewise, sedimentation rates of S1, S2, and residual carbon (RC) fractions showed no difference between disturbed lakes and undisturbed lakes (S1: Disturbed: 0.11 ± 0.12 SD g m^{-2} y^{-1} , Undisturbed: 0.18 ± 0.12 SD g m^{-2} y^{-1}, $t_{(2),12}$ = 1.15, p = 0.27; S2: Disturbed: 3.09 ± 2.27 SD g m^{-2} y^{-1}, Undisturbed 3.07 ± 1.89 g m^{-2} y^{-1}, $t_{(2),12}$ = 0.012, p = 0.99; RC: Disturbed: 11.6 ± 6.22 g m^{-2} y^{-1}, Undisturbed: 10.9 ± 4.1 SD g m^{-2} y^{-1}, $t_{(2),12}$ = 0.23, p = 0.81). This apparent 'dilution' of organic carbon by inorganic sediments was further evident by the inverse correlation between total organic carbon concentration and sedimentation rate (r = 0.66, $F_{1,12}$ = 9.3, p=0.01, Figure 2.2A). Disturbed lakes had significantly lower total organic carbon content and higher sedimentation rates, suggesting that accelerated

deposition of inorganic sediments from retrogressive thaw slumps diluted the sedimentary organic carbon. This inorganic sediment dilution effect was evident for other organic fractions as well (e.g. S2, Figure 2.2B).

2.4.3-Mercury in surface sediments

Mercury concentration in surface sediments was significantly correlated with total organic carbon ($r=0.73$, $p<0.05$, Figure 2.3A), and S2 carbon ($r=0.60$, $p<0.05$, Figure 2.3B) but not as strongly related toinferred chlorophyll *a*($r=0.50$, $p=0.06$, Figure 2.3C). The strong relationship between Hg, TOC and S2 indicates their important role in adsorbing Hg and depositing it to sediments. Likewise, there was a significant correlation between Hg and RC in surface sediments ($r=0.77$, $p=0.001$). RC partially represents the quantity of thermally resistant organic material, which only decomposes during high temperature oxidation such as in forest fires and domestic wood burning, which may partly explain the correlation between the Hg and RC (Goodarzi et al., 2006).

Likewise, methyl mercury in surface sediments was significantly correlated to total organic carbon ($r=0.78$, $p<0.01$, Figure 2.4), S1 carbon ($r=0.71$, $p<0.01$), and S2 carbon ($r=0.79$, $p<0.05$), indicating an important association between methyl mercury formation and organic carbon , and suggest organic matter was a controlling factor which is in turn influenced by permafrost status in these lakes. Taken together, the results suggest that dilution of organic matter by rapid influx of inorganic sedimentation in thaw slump lakes (Figure 2.2) reduces mercury and methyl mercury concentrations in these sediments.

Mercury concentrations in surface sediments in undisturbed lakes were higher (0.12-0.30 µg/g dw) than disturbed lakes (0.07-0.12 µg/g dw), ($t = 4.99$, $p<0.01$). Mercury concentration

was correlated with sedimentation rate in undisturbed lakes (R^2=0.89, p<0.05, Figure 2.2) but no correlation was found in disturbed lakes, which might be due to differences in thaw slump activity among disturbed lakes. An inverse correlation was found between sedimentation rate and mercury in our study lakes (R^2=0.68, P<0.01, Figure 2.5).

Mercury concentrations in disturbed lakes were comparable to other studies in the Canadian Arctic (Carrie et al.,2010, Muir et al., 2009, Stern et al., 2009), but were generally higher in undisturbed lakes, except in 14a. There was no difference in focus corrected mercury fluxes between undisturbed lakes (25.35 ± 3.01µg $m^{-2}y^{-1}$) and disturbed lakes 26.61 ± 6.92 µg $m^{-2}y^{-1}$). Temporal analysis (Deison thesis, Chapter 3) on Hg fluxes in sediment profiles of 8 of our study lakes showed Hg increases at the surface of all study lakes except 2a and 9b.($\Delta Hg F_F$ -69-66 µg $m^{-2}y^{-1}$). In order to estimate the Hg influx from catchment erosion, and in our case sources such as permafrost degradation, HgF_F values were adjusted for post-1850 changes in sedimentation rate to obtain $HgF_{F,adj}$ following the methods of Muir et al. (2009). Average $HgF_{F,adj}$ values (-139-0.03 µg $m^{-2}y^{-1}$) were lower than F_F values for our study lake suggesting inputs of Hg from the catchment (Table 2.2).

MeHg in surface sediments (0-5 cm) from all six undisturbed lakes (0.94±0.54ng g^{-1}d.w.) was substantially higher than in disturbed lakes (0.35±0.20 ng g^{-1}dw, $t_{(2),\ 13}$ = 3.28, p=0.01, Table 2.2, Figure 2.4). We also found a strong correlation between THg and MeHg in surface sediments (r=0.88, p=0.01), suggesting that Hg methylation may be Hg-limited.

2.4.4-S2 Carbon and Inferred Chlorophyll a in Surface Sediments

Average inferred chlorophyll *a* concentration in surface sediments of undisturbed lakes (0.034 ± 0.017 mg g^{-1} DW) was slightly higher than their paired reference lakes (0.019 ± 0.019 017 mg g^{-1} DW) but was not statistically different($t=1.70$, $p>0.05$). Algal-derived OC or S2 in surface sediments was significantly correlated to inferred chlorophyll *a* ($r=0.83$, $p<0.0002$, Figure 2.6). This would be expected because S2 is primarily of algal origin and sedimentary inferred chlorophyll *a* is also typically of autochthonous origin (Michelutti et al. 2010, and papers cited therein).

2.4.5-Organic Carbon in Surface Sediments

Source and composition of organic matter is presented by plotting the quantity of S2 as a function of TOC (Figure 2.7), representing the proportion of hydrogen-rich organic matter dominantly composed of autochthonous (mainly algal-derived) matter relative to the total organic carbon in the sediments (Langford and Blanc-Valleron 1990). Kerogens showing highest S2/TOC are classified as Type I, with Type II and Type III having descending S2/TOC values (Tissot et al., 1974). Sedimentary OM in the majority of surface sediments in all lakes were classified as Type II and III kerogen, whether or not they were disturbed by thaw slumps (Figure 2.7), suggesting a predominantly allochthonous source of organic matter to sediments of all lakes regardless of permafrost status (Figure 2.7A).

Similarly, the organic matter composition may be further characterized by hydrogen content as shown by hydrogen index (HI) and oxygen index (OI) parameters. HI is calculated by

normalizing the quantity of S2 to total organic carbon (S2/TOC x 100), and is proportional to the kerogen elemental H/C ratio (Espitalié et al., 1977). OI, calculated as S3/TOC x 100, is proportional to the elemental O/C ratio of the kerogen (Espitalié et al., 1977). Kerogens of dominantly autochthonous (algal) origin are known to have elevated HI (hydrogen-rich) values relative to terrestrially-derived, reworked organic matter, and plot in Type I and II kerogen space of the S2:TOC plot (Van Krevelen, 1961). All surface sediments plotted in Type III kerogen space on the Van Krevelen diagram (Figure 2.7B), further corroborating evidence that the majority of organic matter in these sediments is of allochthonous origin.

2.5-Conclusions

Radiometrically dated sediment cores from 14 thermokarst lakes in the Mackenzie Delta uplands (i.e. 7 with permafrost thaw slumps (denoted 'b') paired with 7 nearby reference lakes (denoted 'a')) were compared to assess the impact of thaw slump development on mercury and organic sedimentation in lakes of the Mackenzie Delta region. The results show that sediments from lakes disturbed by thaw slump development contained lower concentrations of total organic carbon and algal derived organic carbon (S2), lower mercury and methyl mercury concentrations, as well as higher total and inorganic sedimentation rates, which likely explain the dilution of organic materials and mercury in lakes where thaw slumps are present. Likewise our results showed significant correlations between mercury and S2 in all our study lakes except one pair (2a and 2b) generally supporting the hypothesis that algal-derived materials may be sources of Hg to sediments.

2.6-Acknowledgments

This study was funded by a Natural Sciences and Engineering Research Council (Canada) Strategic Projects grant to JMB, JPS, and MFJP. Logistical support was provided by the Polar Continental Shelf Program (PCSP). We thank Peter deMontigny for field assistance.

References

ACIA. 2005. Arctic Climate Impact Assessment. *Cambridge University Press*, Cambridge, UK. pp. 1042.Appleby, P. 2001. Chronostratigraphic techniques in recent sediments. In: Tracking Environmental Changes in Lake Sediments: *Physical and Chemical Techniques*. Last, W.M. and Smol, J.P. (Eds.) Kluwer Academic Publishers, Dordrect.

Bloom NS, Gill GA, Cappellino S, Dobbs C, McShea L, Driscoll C, Mason R, Rudd J: Speciation and cycling of mercury in Lavaca Bay, Texas, sediments. *Environmental Science & Technology* 1999, 33(1):7-13.

Braddock, J.F., McCarthy, K.A. 1996. Hydrologic and microbiological factors affecting persistence and migration of petroleum hydrocarbons spilled in a continuous permafrost region. *Environmental science and Technology* 30: 2626-2633.

Brigham ME, Krabbenhoft DP, Olson ML, DeWild JF. 2002. Methylmercury in flood-control impoundments and natural waters of northwestern Minnesota, 1997-99. *Water Air Soil Pollut*. 138: 61-78.

Burn CR. 2002. Tundra lakes and permafrost, Richards Island, western Arctic coast, Canada. *Can. J. Earth Sci*. 39: 1281-1298.

Carey SK. 2003. Dissolved organic carbon fluxes in a discontinuous permafrost subarctic alpine catchment. *Permafrost and Periglacial Processes* 14: 161-171.

Carrie J, Wang F, Sanei H, Macdonald RW, Outridge PM, Stern GA. 2010. Increasing contaminant burdens in an Arctic fish, burbot (*Lotalota*), in a warming climate. *Environ. Sci. Technol.* 44 : 316-322.

Curtosi, A., Pelletier, E., Volopiez, C.L., MacCormack, W.P. 2007. Polycyclic aromatic hydrocarbons in soil and surface marine sediment near Jubany Station (Antarctica). Role of permafrost as a low-permeability barrier. *Sci. Tot. Environ*. 383: 193-204.

Davis N. 2001. Permafrost: a guide to frozen ground in transition. University of Alaska Press, Fairbanks, AK. pp. 351.Lachenbruch and Marshall 1986,

Glew JR, Smol JP, Last WM. 2001. Sediment core collection and extrusion. In Basin Analysis, Coring, and Chronological Techniques; Last WM, Smol JP, Eds.; Kluwer Academic Publisher: Norwell 73-106.

Espitalié J, Laporte J-L, Madec M et al (1977) Méthode rapide de caractéristique des roches mères, de leur potentiel pétrolier et de leur degré d'évolution. Revue de l'Institut français du Pétrole, 32: 23-42.

Glew JR. 1988. A portable extrudingdevice for close intervalsectioning of unconsolidatedcoresamples. J. Paleolimnol. 2(3): 241-243.

Goodarzi, F., Reyes, J., Schulz, J., Hollman, D., Rose, D., 2006. Parameters influencing the variation in mercury emissions from an Alberta power plant burning high inertinite coal over

38 weeks period. Int. J. Coal Geol. 65, 26–34.

Hintelmann H, Wilken RD: Levels of Total Mercury and Methylmercury Compounds in Sediments of the Polluted Elbe River - Influence of Seasonally and Spatially Varying Environmental-Factors. *Science of the Total Environment* 1995, 166(1-3):1-10.

Hobbie, J.E., Peterson, B.J., Bettez, N., Deegan, L., O'Brien, W.J., Kling, G.W., Kipphut, G.W., Bowden, W.B., et al. 1999. Impact on global change on the biogeochemistry and ecosystems of an arctic freshwater system. Polar Res. 18, 207–214.

Jorgenson MT, Shur YL, and Pullman ER. 2006. Abrupt increase in permafrost degradation in Arctic Alaska. *Geophys*. Res. Let. 33: L02503.

Kokelj, S.V., Burn, C.R. 2005. Near-surface ground ice in sediments of the Mackenzie Delta, Northwest Territories, Canada. *Permafrost and Periglacial Processes* 16: 291-303.

Kokelj SV, Jenkins RE, Milburn D, Burn CR, Snow N. 2005. The influence of thermokarst disturbance on the water quality of small upland lakes, Mackenzie Delta Region, Northwest Territories, Canada. *Permafrost and Periglacial Processes* 16: 343-353.

Lafargue E, Espitalite J, Marquis F, Pillot D. 1998. Rock-Eval 6 applications in hydrocarbon exploration, production and soil contamination studies. *Rev. French Petroleum Inst*. 53:421–437.

Langford FF, Blanc-Valleron MM (1990) Interpreting Rock-Eval pyrolysis data using graphs of pyrolyzable hydrocarbons vs. total organic carbon. *American Association of Petroleum Geology Bulletin* 74: 799-804.

Larter SR, Horsfield B (1993) Determination of structural components of kerogens by the use of analyticalpyrolysis. *Inorganic Geochemistry* (Edited by Engel M.H. and Macko S.A.), pp. 271-287. Ch.13, Plenum Press.

Macdonald RW, Harner T, Fyfe J. 2005. Recent climate change in the Arctic and its impact on contaminant pathways and interpretation of temporal trend data. *Sci. Tot. Environ*. 342: 5-86.

Macdonald RW and Loseto LL, 2010. Are Arctic Ocean ecosystems exceptionally vulnerable to global emissions of mercury? A call for emphasized research on methylation and the consequences of climate change. *Environmental Chemistry*, 7: 133-138.

McGuire AD, Macdonald RW, Schuur EAG, Harden JW, Hayes DJ, Christensen TR and Heimann M. 2010. The carbon budget of the northern cryosphere region. *Current Opinion in Environmental Sustainability in press*.2010, 2:231–236

Muir,D.C.G.;Wang, X.; Yang, F.;Nguyen,N.; Jackson, T.; Evans, M.;Douglas,M.;Ko ¨ck,G.; Lamoureux, S.; Pienitz,R.; et al. Spatial trends and historical deposition of mercury in eastern and northern Canada inferred from lake sediment cores. *Environ. Sci. Technol*. 2009, 43, 4802–4809.

Michellutti, N., Blais, J.M., Cumming, B.F., Paterson, A.M., Rühland, K., Wolfe, A.P., Smol, J.M. 2010. Do spectrally inferred determinations of chlorophyll *a* reflect trends in lake trophic status? *Journal of Paleolimnology* 43: 205-217.

Michelutti,N., Wolfe, A. P., Vinebrooke, R.D. and Rivard, B.2005. Recent primary production increases in Arctic lakes. Geophysical Research Letters. 32: L19715, doi:10.1029/2005 GL023693.

Omelchenko A, Lockhart WL, Wilkinson P. 1995. The depositional characteristics of lake sediments across Canada as determined by ^{210}Pb and ^{137}Cs. Unpublished Internal Report, Freshwater Institute: Winnipeg, 48 pp.

Outridge PM, Sanei H, Stern GA, Hamilton PB, Goodarzi F. 2007. Evidence for control of mercury accucmulation rates in Canadain High Arctic lake sediments by variations of aqatic primary productivity. *Environ. Sci. Technol*. 41: 5259-5265.

Pavlov AV. 1994. Current changes of climate and permafrost in the Arctic and Sub-Arctic of Russia. *Permafrost Periglac. Process*. 5: 101-110.

Perry, E.; Norton, S. A.; Kamman, N. C.; Lorey, P. M.; Driscoll, C. T., Deconstruction ofhistoric mercury accumulation in lake sediments, northeastern United States. *Ecotoxicology*2005, 14, 85-99.

Pickhardt PC, Folt CL, Chen CY, Klaue B, Blum, JD. 2002. Algal blooms reduce uptake of toxic methylmercury in freshwater food webs. *Proceedings of the National Academy of Sciences* 99: 4419-4423.

Prowse TD, Wrona FJ, Reist JD, Gibson JJ, Hobbie JE, Lévesque LMJ, and Vincent WF. 2006. Climate change effects on hydroecology of Arctic freshwater ecosystems. *Ambio* 35: 347-358.

Sanei H, Stasiuk LD, Goodarzi F. 2005. Petrological changes occurring in organic matter from recent lacustrine sediments during thermal alteration by Rock-Eval pyrolysis. *Org. Geochem*. 36: 1190–1203.

Serreze MC, Walsh JE, Chapin III FS, Osterkamp T, Dyurgerov M, Ramanovsky V, Oechel WC, Morison J, Zhang T, and Barry RG. 2000. Observational evidence of recent change in the northern high-latitude environment. *Climatic Change* 46: 159-207.

Smol JP, Douglas MSV. 2007. From controversy to consensus: making the case for recent climatic change in the Arctic using lake sediments. Frontiers in Ecology and the Environment 5: 466-474.

Stern GA, Braekevelt E, Helm PA, Bidleman TF, Outridge PM, Lockhart WL, McNeely R, Rosenberg B, Ikonomou MG, Hamilton MG, Tomy GT, Wilkinson P. 2005. Modern and historical fluxes of halogenated organic contaminants to a lake in the Canadian Arctic, as determined from annually laminated sediment cores. *Sci. Tot. Environ*. 342: 223-243.

Stern, G. A.; Sanei, H.; Roach, P.; De La Ronde, J.; Outridge, P. M. Historical interrelatedvariations of mercury and aquatic organic matter in lake sediment cores from a subarctic lake inYukon, Canada: Further evidence toward the algal-mercury scavenging hypothesis. *Environ. Sci. Technol*. 2009, 43, 7684–7690.

St Louis VL, Rudd JWM, Kelly CA, Bodaly RA, Paterson MJ, Beaty KG, Hesslein RH, Heyes A, Majewski AR. 2004. The rise and fall of mercury methylation in an experimental reservoir. *Environ. Sci. Technol*. 38: 1348-1358.

Sunderland EM, Gobas F, Heyes A, Branfireun BA, Bayer AK, Cranston RE, Parsons MB: Speciation and bioavailability of mercury in well-mixed estuarine sediments. *Marine Chemistry* 2004, 90(1-4):91-105.

Tissot B, Durand B, Espitalié J et al (1974) Influence of the nature and diagenesis of organic matter in the formation of petroleum. *AmerAssoc Petrol Geol Bull* 58: 499-506.

Ullrich SM, Tanton TW, Abdrashitova SA: Mercury in the aquatic environment: A review of factors affecting methylation. Critical Reviews in *Environmental Science and Technology* 2001, 31(3):241-293.

Van Krevelen DW (1961) Coal. Typology, chemistry, physics, constitution. Elsevier, New York.

Wolfe, A. P., Vinebrook, R. D., Michelutti, N., Rivard, B. And Das, B. 2006. Experimental calibration of lake-sediment spectral reflectance to chlorophyll *a* concentrations: methodology and paleolimnological validation. Journal of Paleolimnology 36: 91–100, doi:10.1007/s10933-006-0006-6.

Table 2.1: Location and physical characteristics of the 14 study lakes located in the uplands directly to the east of the Mackenzie River Delta NWT, Canada. Morphometric data and slump activity were determined from air photo analyses and ground surveys undertaken during 2001–2005 (Kokelj et al. 2005).

Lake	Latitude (°N)	Longitude (°W)	A_o[1] (ha)	CA[2] (ha)	SA[3] (ha)	Slump status	Z_m[4] (m)	FF[5]	Average Sed. Rate[6] ($g\ m^{-2}y^{-1}$)
	I. Undisturbed Lakes								
2a	68°50' 26.7"	133° 66' 07.1"	2	17.2	–	–	6.1	2.30	67
5a	68°33'4.20"	133°38'23.39"	2.9	20.9	–	–	10.9	0.96	132
6a	68°35'25.73"	133°38'33.40"	3.6	19.7	–	–	2.3	0.94	121
7a	68°36'18.47"	133°35'27.14"	1.4	18.1	–	–	2.7	2.45	34
9a	68° 58' 05.8"	133° 53' 53.0"	3.1	29.3	–	–	2.7	4.57	20
14a	68° 31' 02.7"	133° 44' 55.4"	3.4	33.5	–	–	7.5	0.87	210
36a	68° 30' 10.4"	133° 42' 02.2"	0.8	6.6	–	–	9.5	0.77	119
	II. Disturbed Lakes								
2b	68° 50' 72.8"	133° 67' 03.6"	4.9	15.9	0.95	Stable	3.4	0.46	556
5b	68°32'14.96"	133°39'27.41"	2.8	27.7	2.02	Stable	9	5.00	61
6b	68°35'17.78"	133°38'16.95"	1.2	7.5	0.81	Stable	2	0.55	528
7b	68°36'32.23"	133°35'12.77"	3.1	34.7	1.13	Active	5	0.89	271
9b	68° 58' 14.1"	133° 53' 59.3"	3.6	7.2	2.5	Active	3	1.18	240
14b	68° 31' 02.7"	133° 44' 55.4"	9.2	45.1	2.4	Active	10.5	0.05	6594
36b	68° 30' 09.6"	133° 42' 05.2"	3.9	24.4	4.9	Stable	7.4	0.51	290

[1]$A_{o=}$ lake surface area

[2]CA= catchment area

[3]SA= area of retrogressive thaw slump

[4]$Z_{m=}$ maximum depth of lake

[5]FF= focusing factor

[6] Sedimentation rate was calculated using the CFCS model (Appleby 2001)

Seven study disturbed lakes have retrogressive thaw slumps (i.e. degraded permafrost) and the other seven lakes are in undisturbed catchments. Disturbed lakes are denoted by the letter b, whereas undisturbed lakes are identified by the letter a.

Table 2.2: Mercury and methyl mercury concentrations in surface sediments from twelve lakes There is no methyl mercury data available for lakes 2a and 2b due to lack of surface sediments.

Sample	Depth (cm)	Core Date	Hg (ng g^{-1} DW)	$HgF_{f,adj}$ (µg $m^{-2}y^{-1}$)	ΔHgF_F (µg m^{-2} y^{-1})	MeHg Concentration (ng g^{-1} DW)
INV07 2a	0.25	2007	182	-92.20	-46.00	
INV08 9a	0.25	2007	265	-0.08	22.00	1.489
INV08 14a	0.25	2007	125	0.03	6.33	1.452
INV08 36a	0.25	2003	308	0.03	66.00	1.327
INV07 5a	0.25	2007	171			0.446
INV08 6a	0.25	2008	257			0.27
INV08 7a	0.25	2008	281			0.683
INV07 2b	0.25	2007	121	0.00	30.00	
INV08 9b	0.25	2007	120	-139.37	-69.75	0.739
INV08 14b	0.25	2008	78	-54.27	-27.00	0.365
INV08 36b	0.25	2003	88	0.03	15.50	0.279
INV07 5b	0.25	2007	99			0.281
INV08 6b	0.25	2008	91			0.227
INV07 7b	0.25	2007	96			0.221

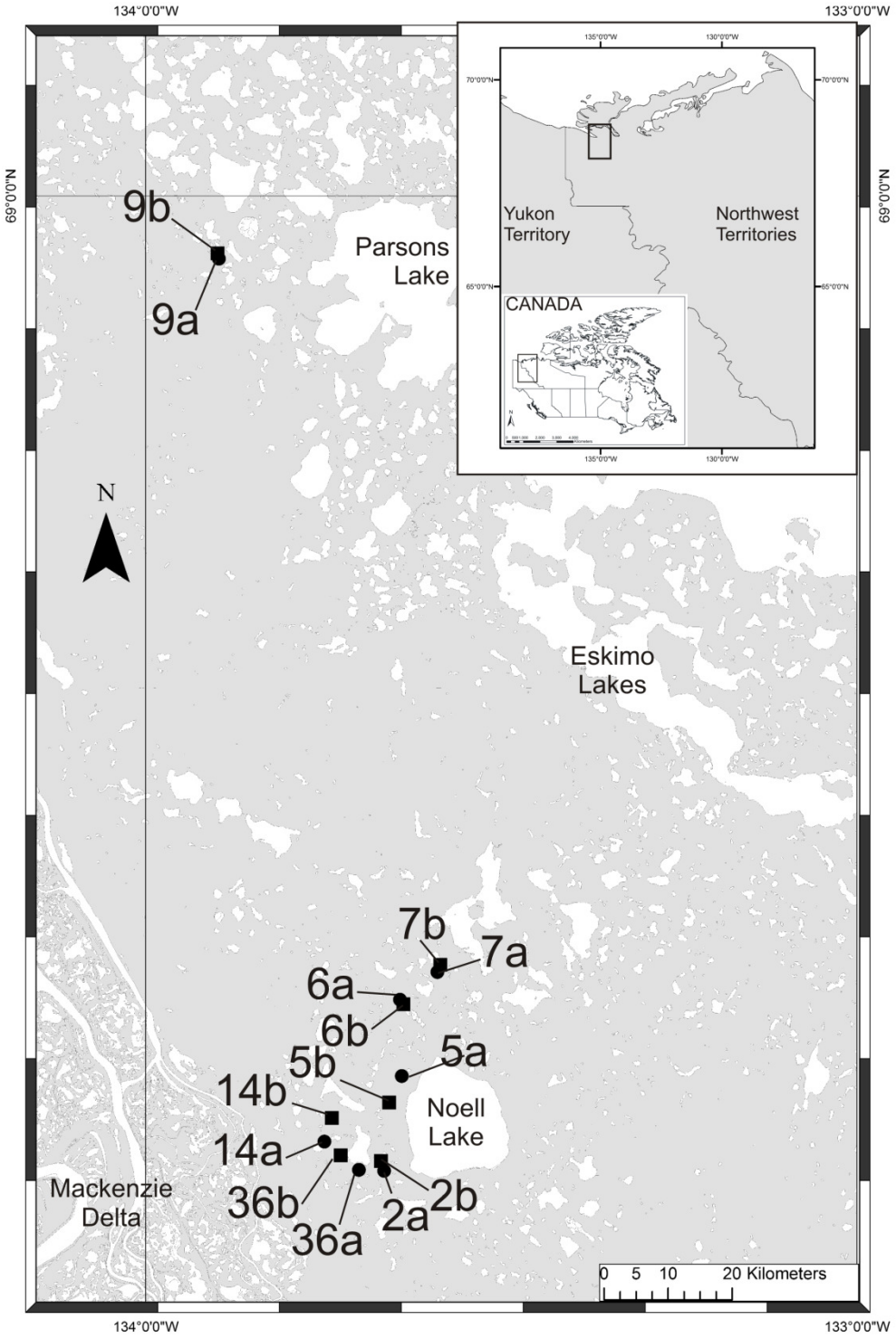

Figure 2.1: Study lakes in the Mackenzie Delta near Inuvik. Lakes denoted 'a' are undisturbed lakes, and those denoted 'b' have catchments disturbed by permafrost melting.

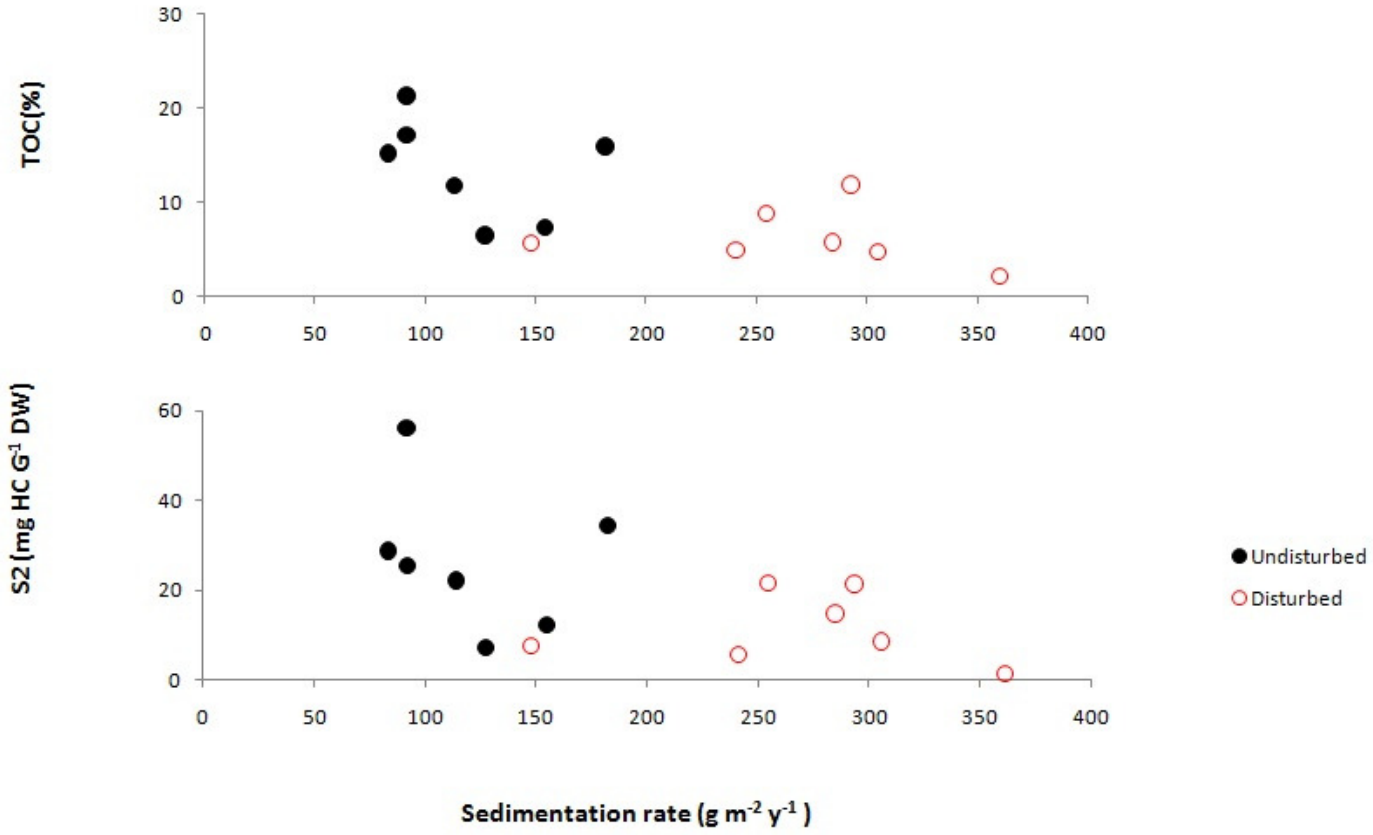

Figure 2.2: Sedimentation rate in sediment cores from 14 study lakes (focus corrected to 50 Bq m^{-2} y^{-1} excess ^{210}Pb) plotted against (A)the total organic carbon in surface sediments , and (B) the S2 (algal derived) carbon in surface sediments . Note that sedimentation rate in disturbed lakes tends to be higher than in undisturbed lakes, and organic carbon is lower and 'diluted' by the higher inorganic sediment flux seen in disturbed lakes.

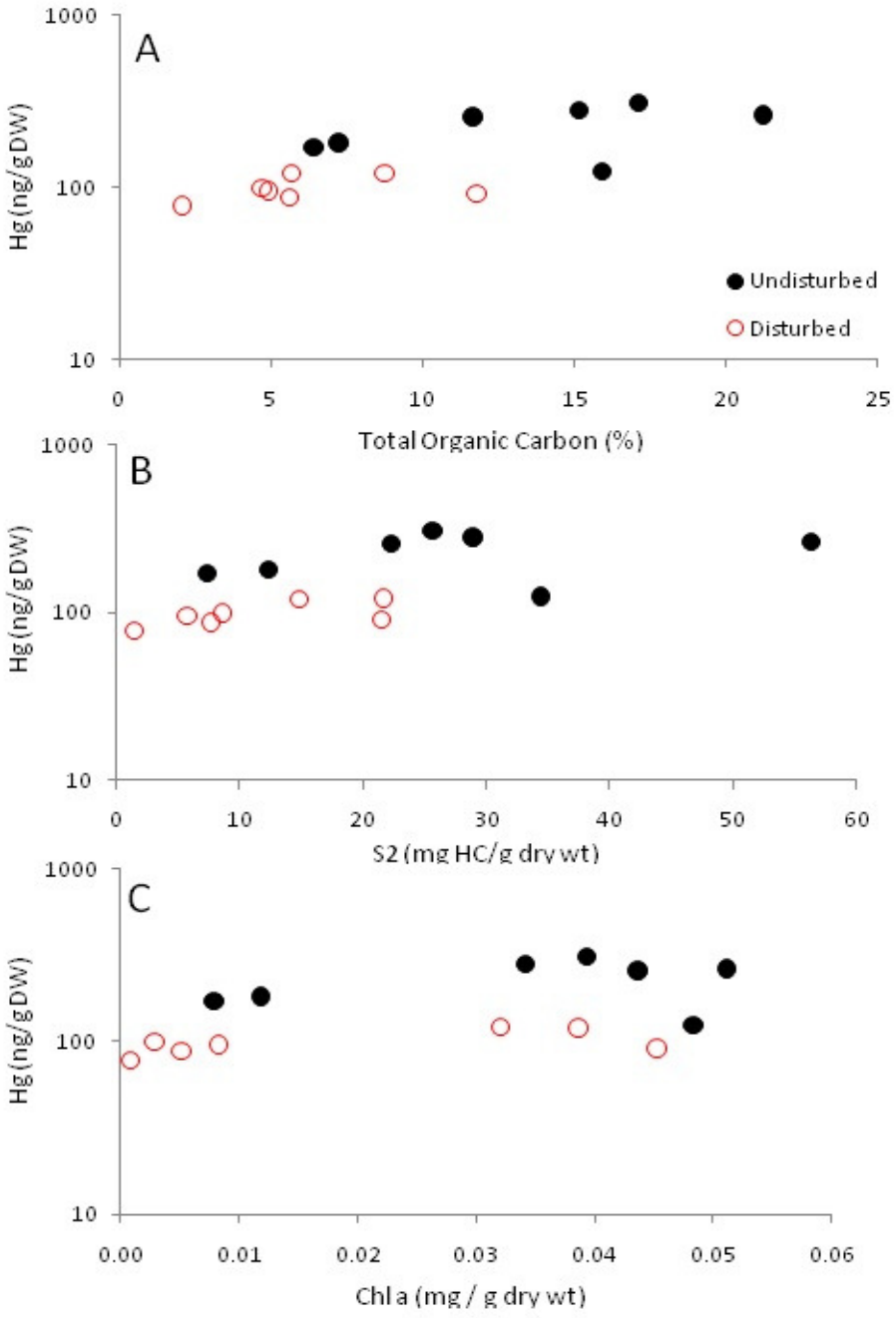

Figure 2.3: Mercury concentrations in surface sedimnents from 14 study lakes plotted against (A) total organic carbon in surface sediments; (B) S2 or algal derived organic carbon in surface sediments, and (C) inferred chlorophyll *a* in surface sediments. All correlations are significant at $\alpha<0.05$.

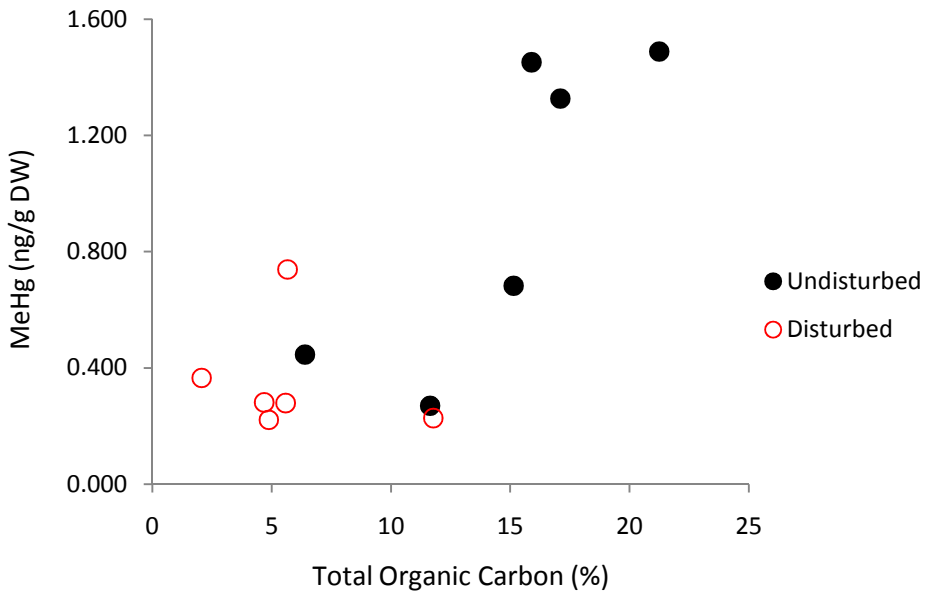

Figure 2.4: Methyl mercury concentrations in surface sediments from 12 separate lakes plotted against the total organic carbon in surface sediments. Twelve lakes are represented here because insufficient surface sediment for methyl mercury analysis was available for two of the 14 study lakes.

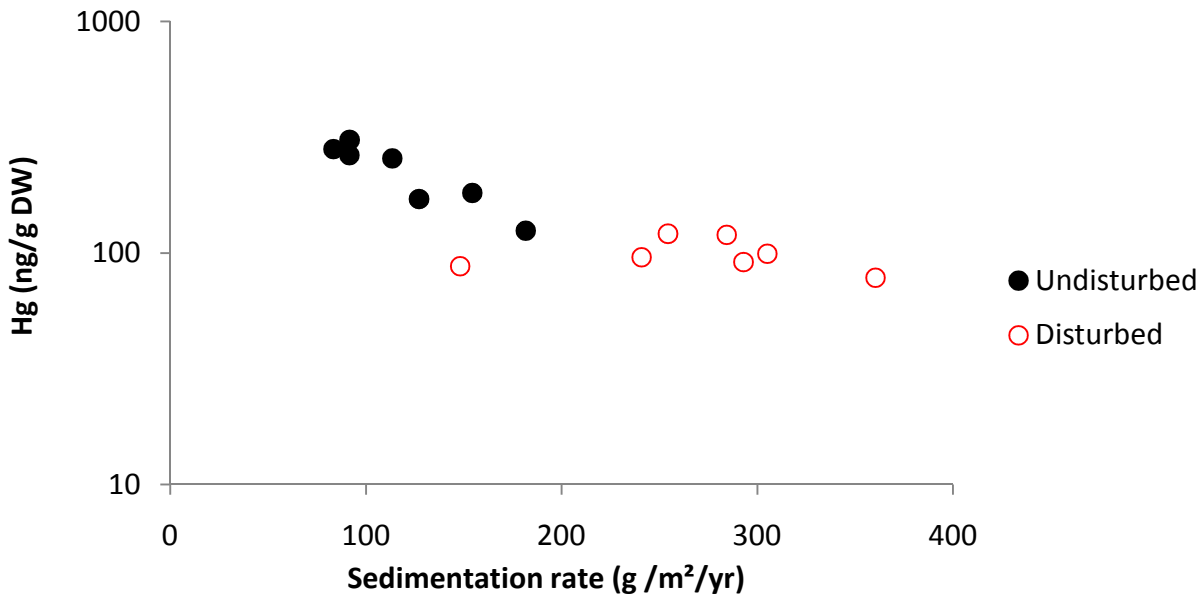

Figure 2.5: Sedimentation rates in sediment cores from 14 study lakes (focus corrected to 50 Bq m^{-2} y^{-1} excess ^{210}Pb) plotted against the mercury concetration in surface sediments. This correlation is significant at $\alpha<0.05$.

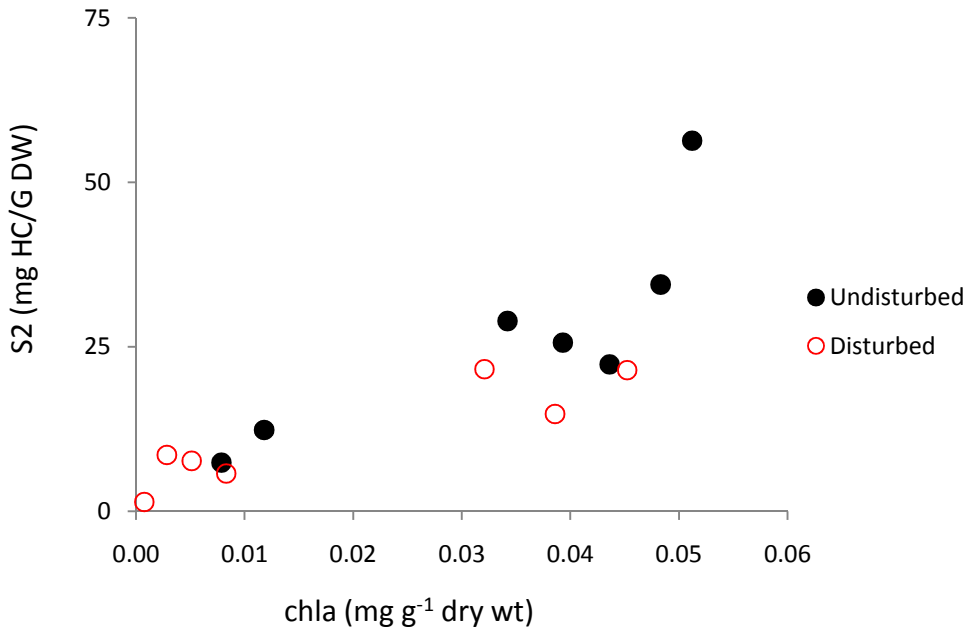

Figure 2.6: S2 (predominantly composed of more stable algal-derived matter) in surface sediment cores from 14 study lakes plotted against the inferred chlorophyll *a* (mg g¹ dry wt) in surface sediments.

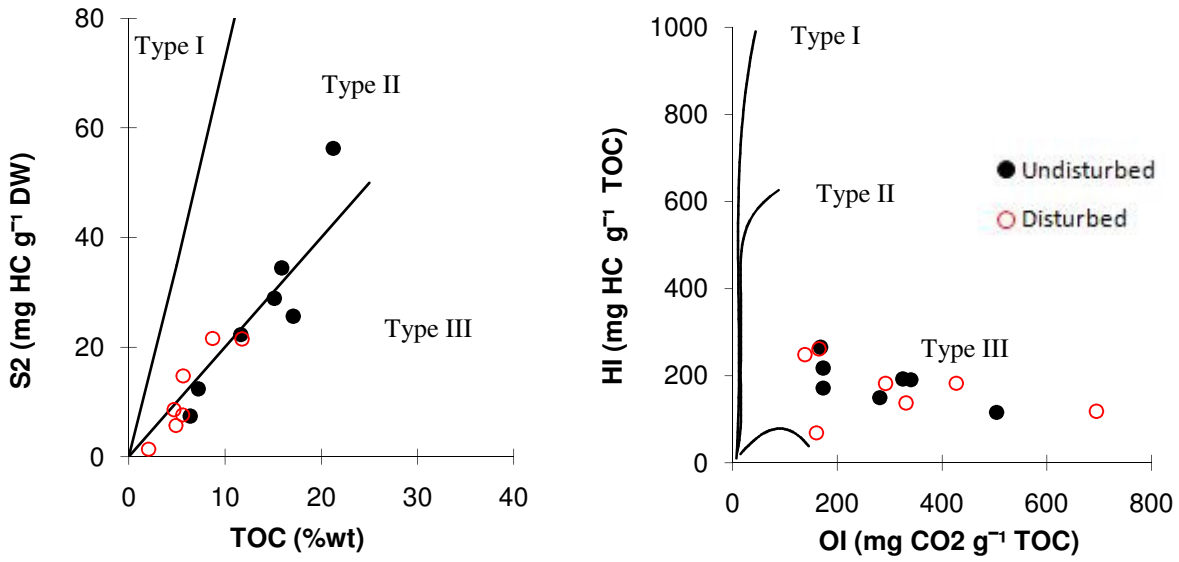

Figure 2.7: Type of organic matter (kerogen) in recent sediments from the Mackenzie Delta region, S2 vs. TOC plot. The solid lines define the boundaries of Type I, II, and III kerogens.

3.0-Temporal assessment of mercury and organic matter in lakes affected by thermokarst in the Mackenzie Delta region, NWT, Canada

Ramin Deison[1*], John P. Smol[2], Steve Kokelj[3], Michael F.J. Pisaric[4], Alex Poulain[1], Hamed Sanei[5], Josh Thienpont[2], Jules M. Blais[1]

Ramin Deison[1]

John P Smol[2]

Steve Kokelj[3]

Michael F.J.Pisaric[4]

Alexandre Poulain[1]

Hamed Sanei[5]

Joshua Thienpont[2]

Jules M. Blais [1]

[1]Program for Chemical and Environmental Toxicology, Department of Biology, University of Ottawa.

[2]Paleoecological Environmental Assessment and Research Lab (PEARL), Department of Biology, Queen's University, Kingston.

[3]Water Resources Division, Indian and Northern Affairs Canada, Yellowknife.

[4]Department of Geography and Environmental Studies, Carleton University, Ottawa.

[5]Geological Survey of Canada, Calgary.

3.1-Abstract

The Mackenzie Delta region of the Northwest Territories, Canada, has experienced rapid climate warming in the past century. One of the major consequences of climate warming in this region has been thawing permafrost. Here we examine how lakes affected by thawing permafrost have experienced changes in mercury (Hg) and organic carbon (OC) deposition by comparing sediment cores from lakes with and without retrogressive thaw slumps on their shorelines. Four of our study lakes had retrogressive thaw slumps along their shorelines (disturbed), while four other lakes were reference lakes (undisturbed) where thaw slumps were absent. Sediment core profiles from disturbed lakes had higher sedimentation rates and lower total Hg and algal derived OC when compared with reference lakes. Total Hg concentrations in profile were correlated with total organic carbon (TOC), algal derived (S2) organic carbon, and sediment inferred chlorophyll *a*content in most cores, showing that autochthonous organic carbon production was related to Hg delivery in these sediments. Temporal correlations between mercury and S2 in all our study lakes except one pair (14a and 14b) generally supported the hypothesis that algal derived materials were important sources of Hg to sediments. We observed higher S2 concentrations in reference lakes than in slump lakes, likely due to lower dilution by flux of inorganic clastic matter. We show that permafrost thaw slump development in the Mackenzie Delta region generally increased sedimentation of inorganic matter in sedimentary archives, diluting organic carbon and Hg in lake sediments.

.3.2-Introduction

Arctic regions have experienced climate warming at double the pace of the rest of the globe (IPCC, 2007). In particular, North America's western Arctic is the most rapidly warming region on Earth (Lantz &Kokelj, 2008), with an increase of up to 8^{o}C in the Canadian Arctic predicted by 2100 (IPCC, 2007). Currently, about one fifth of the exposed surface of the Earth is underlain by some form of permafrost, including 22% of the land area in the Northern Hemisphere (Davis 2001). Permafrost covers an area of 26 million km^2 globally (ACIA, 2005), 50% of Canada and 85% of Alaska (Ming-Ko*et al.*, 1992; Jorgenson & Osterkamp, 2005). Permafrost temperatures have been rising due to atmospheric warming, resulting in an increased frequency of terrain disturbances due to the thawing and settling of ice rich terrain (Jorgenson *et al.*, 2006) which can significantly affect local water quality even if they only occupy 2% of a lake's catchment area (Kokelj*et al.*, 2005).

Recent studies have shown that the influx of slump material into freshwater systems bring sediment, nutrients, and organic carbon which were trapped in the frozen soil and ice (Macdonald et al., 2005). These alterations are likely to change the amount of metallic and organic contaminants entering freshwater lakes, but there is a significant gap in our knowledge of how ecosystems will respond to climate warming in thermokarst regions.

Previous studies of mercury from hydroelectric reservoirs showed that rapid decomposition and oxygen depletion in soils resulted in increased mercury and methyl mercury release to surface waters (St-Louis et al. 2004, Brigham et al. 2002), though comparable information for permafrost has not been collected. Mercury contamination has been observed in remote areas such as the Arctic, and as such, it has become known as a global pollutant (Ariya et

al., 2004). It is estimated that 60% of atmospheric mercury is deposited on land and 40% on water and in the Arctic. Most of the land-deposited mercury is likely to enter aquatic environments through melt-water and runoff (Macdonald et al., 2005). Likewise, some studies on contaminated soils show that continuous permafrost typically acts as an effective barrier preventing contaminants from infiltrating into the ground (e.g. Braddock and McCarthy 1996), and some (e.g., Curtosi et al. 2007) have predicted that thawing permafrost will release contaminants to surface waters, with unknown ecological consequences.

Another important consideration has been increased algal productivity from pronounced climate warming in Arctic lakes, which may also increase contaminant delivery to lake sediments (Macdonald et al. 2005, Stern et al. 2005, Outridge et al. 2007, Stern et al., 2009, Carrie et al. 2010, Sanei et al. 2010). Variations in the source, type, and relative quantity of autochthonous versus allochthonous organic matter have been suggested to affect the delivery of mercury to aquatic systems (Jackson 1986; Kainz et al. 2003; Sanei and Goodarzi, 2006). In addition, a number of recent studies on northern lakes have reported similarities in temporal trends of mercury and S2 (algal-derived)organic matter (Outridge et al. 2007; Carrie et al. 2009; Stern et al. 2009). These studies suggested that algal-derived carbon is primarily responsible for mercury scavenging in the water column and this effect is likely on the rise in recent decades due to climate-related increases in algal productivity due to climate warming, especially during the past several decades. On the other hand, another recent study conducted by Kirk et al. (2011) showed that algal scavenging does not always explain Hg deposition to sediments adequately, based on a broad survey of lake sediment cores across the Canadian Arctic.

Nevertheless, the algal scavenging hypothesis may offer one explanation for mercury increases in Arctic lake sediment archives despite decreasing atmospheric mercury concentrations (Fain et al. 2009; Li et al. 2009).

The primary objective of this study was to examine mercury and organic matter sediment profiles in lakes affected by thawing permafrost in a case-control analysis where retrogressive thaw slumps were present and absent (Figure 3.1). We predicted, based on an earlier spatial assessment of surface sediments in this thermokarst region, that sediment cores from lakes disturbed by thawing permafrost would have higher inorganic sedimentation rates, lower total Hg concentration, and lower total organic carbon and S2 organic carbon content than reference lakes where thaw slumps were absent. We investigated whether the history of permafrost thaw slump development could be reconstructed from lake sediment cores. We also predicted that, within each sediment profile, Hg would correlate with S2 carbon as predicted by the algal scavenging hypothesis.

3.3-Methods

3.3.1-Study Area

Eight sediment cores used for this study were obtained from eight lakes along a transect east of the Mackenzie Delta, from Inuvik to Richards Islands (Figure 3.1). These lakes were chosen following an analysis of aerial photographs and field surveys (Kokelj et al. 2005). Four study lakes have retrogressive thaw slumps on their shorelines (disturbed lakes) and are denoted by the letter b and the other four lakes are in undisturbed catchments and are denoted by letter a. The location and characteristics of the study lakes are given in Table 3.1.

3.3.2-Sample Collection and Preparation

Eight sediment cores measuring 35-40 cm in length were recovered from the centre of the eight lakes in summer 2007-2008 using a Glew corer and Plexiglas core tubes (Glew 1988). All the cores were sub-sampled at 0.25 cm intervals between 0 and 15 cm and at 0.5 cm intervals from 15 cm to the bottom with a core extruder (Glew et al. 2001). The sediment samples were placed into air-tight centrifuge tubes and plastic bags, placed on ice, and transported in a dark cooler to the laboratory the same day. Sediments were then stored in a freezer for future analysis. The sediments were sub-sampled and freeze-dried for 2 to 3 days, and the dried sediments were ground for radiometric analysis, THg, and inferred chlorophyll *a*content and Rock-Eval analysis.

3.3.3-Total Mercury in Sediments

Homogenized freeze-dried sediment samples were analyzed for total mercury using an automatic Mercury Analyzer based on thermal decomposition, dual step gold amalgamation and detection via Cold-Vapor Atomic Absorption using a Sp-3D mercury analyzer (Nippon instrument Corp) with detection limit of 0.01ng per sample size. Sample mass ranged between 25-30 mg. The accuracy of our analysis was estimated by running blanks and spikes as well as Reference Material (MESS-3) during the analytical procedure. Spikes from a stock of Mercury Reference Solution (certified 1000 $\mu g\ g^{-1}$ ± 1 %; Fisher Scientific CSM114-100) were brought to a concentration of 50 $ng\ g^{-1}$ and were tested every 5 samples. The average recovery of the spikes was 102 % ± 5(SD), (n = 12). According to procedural blanks, no contamination was observed during THg analysis. Reference Materials were tested every 4-5 samples and average percentage recovery for MESS-3 (Marine Sediment Certified Reference Materials from NRC with concentration of 91 ± 9 $ng\ g^{-1}$ was 96 % ± 4 (SD), (n = 35).

3.3.4-^{210}Pb Inventories and Sedimentation Rates

Sediment cores were radiometrically dated using gamma (γ) spectrometry. The eight sediment cores were analyzed for ^{210}Pb, ^{137}Cs and ^{226}Ra activity. Analysis of ^{210}Pb was performed at 12-15 selected depth intervals in the sediment cores to determine sediment age and sediment accumulation rate. Samples were ground and homogenized, then added to centrifuge tubes (8.4 cm high and 1.5 cm outer diameter) to a height of 2 cm. Sediment samples were settled for a minimum of two days before sealing with an epoxy resin. Sealed samples were left to reach secular equilibrium for a minimum of 3 weeks, then counted using a digital high purity germanium well detector (DSPec, Ortec), following the method in Appleby (2001). Samples were counted for 23 hours (82,800 seconds). The resulting spectrum files showed ^{210}Pb activity with a peak at 46.5 keV, and ^{137}Cs at 662 keV. ^{226}Ra activity was determined by γ-ray emissions of its daughter isotope ^{214}Pb, resulting in peaks at 295 and 352 keV.

^{210}Pb and ^{137}Cs were performed to date the sediment cores by gamma spectrometry, using a digital high purity germanium well detector (DSPec, Ortec), following the method described by Appleby (2001).Long term sedimentation rates were determined for each core using the constant rate of supply (CRS) (Appleby and Oldfield 1978).^{137}Cs activity (from atmospheric fallout of nuclear weapons, peaking in 1963) was measured to verify ^{210}Pb dates. Focus factors (FF) were determined by dividing the deposition rate of excess ^{210}Pb in each sediment core [excess ^{210}Pb inventory (Bq m^{-2}) x ^{210}Pb decay constant (0.03114 yr^{-1})] by the estimated atmospheric excess ^{210}Pb deposition rate at this latitude (50 Bq m^{-2} yr^{-1}, Omelchenko et al. 1995). Fluxes such as Hg flux (HgF), anthropogenic Hg fluxes (ΔHgF), enrichment factors (EFs) , as well as Hg fluxes

adjusted for sedimentation and an adjusted anthropogenic Hg flux ($\Delta F_{F,adj}$; calculated using the equation of Perry et al., 2005) were calculated as follows:

5) F ($\mu g\ m^{-2}\ y^{-1}$) = Concentration ($\mu g\ g^{-1}$) x ^{210}Pb-derived sedimentation rates ($g\ m^{-2}\ y^{-1}$)

6) ΔF ($\mu g\ m^{-2}\ y^{-1}$) = F_{recent} (post-1990) - $F_{pre\text{-}ind}$(pre-industrial; pre-1850

7) EF= recent (post-1850)/pre-industrial Hg concentrations

8) $\Delta F_{F,adj} = F_{Frecent} - F_{Fpre\text{-}ind} - (F_{Fpre\text{-}ind}$x sedimentation ratio- $F_{Fpre\text{-}ind})$

3.3.5-Organic Geochemistry (Rock-Eval Analyses)

We applied Rock-Eval® 6, (Vinci Technologies, France) for the quantitative and qualitative study of OM in the recent sediments. The Rock-Eval® 6 method consists of pyrolysis (under inert conditions) and then oxidation, both performing a temperature programmed heating of the sediments (30-50 mg) at a rate of 25^{o}C per minute.

The analytical method involves placing the dried sediment sample into a pyrolysis chamber under inert, oxygen-free atmosphere (either helium or nitrogen) and heating it from 300-650°C. S1 and S2 are analyzed by flame-ionization detection (FID) and measured as mgHC/g (HC = hydrocarbons). S3 is measured by infrared (IR) detection, and determines $CO_2$and CO emitted from the sample, and is measured as mg CO_2/g (or mg CO/g). Rock Eval 6 analysis also provides measures of hydrogen index(HI) and Oxygen index (OI) expressed as mg

HC g^{-1} TOC and mg CO_2 g^{-1} TOC respectively, which are indicative of kerogen type (La Fargue et al. 1998; Peters et al. 2005).

The S1 fraction consists of volatile short chain hydrocarbons, pigments, and some humic substances, and is released due to initial thermal de-volatilization of highly labile and volatile organic compounds including some pigments, organic acids, and bio-lipids. The S2 fraction is released due to thermal cracking of kerogen and consists of higher molecular weight aliphatic hydrocarbons corresponding to the biomolecular structure of algal cell walls (Lafargue et al. 1998, Sanei et al. 2005). The S2 fraction is commonly referred to as the 'algal derived' fraction (Outridge et al. 2007, Stern et al. 2009, Carrie et al. 2010). S3 represents CO_2 produced during pyrolysis and consists of oxygen-containing organic compounds, typically from higher plants and terrestrially-derived organic matter. Because of the difficulty in determining precise sources of S3, it has not been used in sediment studies, and will not be considered here. The pyrolyzable carbon (PC) is equal to the sum of S1, S2 and S3 fractions. The refractory organic carbon (residual carbon; RC) is released only after high temperature (400-850°C) incineration of remaining organic matter in presence of oxygen, immediately following the pyrolysis stage. It is composed mostly of highly resistant OM, such as lignins and cellulosic materials from higher plants, and char. It is measured by infrared (IR) detection. Total organic carbon (TOC) is sum of the PC and RC in a given sample (Lafargue et al., 1998; Behar et al., 2001).

3.3.6-Inferred Chlorophyll a in Sediments

Sedimentary chlorophyll *a* content was inferred using visible reflectance spectroscopy (VRS), a method that provides an indication of overall lake production (Michelutti et al. 2005). Samples were freeze dried, sieved (125 µm), and analyzed on a FOSS NIRSystems Model 6500 rapid content analyzer. The portion of the electromagnetic spectrum from 650-700 nm was analyzed in order to detect both chlorophyll *a* and its derivatives (pheophytin*a* and pheophorbide*a*), allowing VRS-chlorophyll *a*to track changed in production over time, and not simply diagenesis (Wolfe et al. 2006, Michelutti et al. 2010).

3.3.7-Statistical Analyses

All data were analyzed usingOrigin Lab 7 software (Origin Lab Corporation MA, USA). Simple linear regressions analysis was used to analyze the relationship between total mercury to S2, inferred chlorophyll *a*, and sedimentation rates. One-way ANOVA was used to test the difference between disturbed and undisturbed lakes with respect to total mercury, S2, inferred chlorophyll *a,*and sedimentation rates.

3.4-Results and Discussion

3.4.1-Sediment core profiles

^{210}Pb activities in most cores declined log-linearly with depth until reaching background, which was determined by secular equilibrium with ^{226}Ra (Figure 3.2). Several cores showed disturbance in their excess ^{210}Pb profiles, particularly in 9b and 14b, suggesting fluctuations in sedimentation at those intervals.

In profile, sedimentary Hg and TOC in reference lakes tended to show modest increases to the surface (Figure 3.3), though not to the same extent as those described in other regions closer to active Hg emissions. Enrichment factors (EF) ranged from 1.27 to 2.50 in lakes 14a and 36a, respectively, which was close to those found throughout the arctic by Kirk et al (1.1-2.6) and others (Cooke et al., 2010; Muir et al., 2009; Stern et al., 2009).

Mercury concentrations in disturbed lakes were comparable to other studies in the Canadian Arctic (Carrie et al.,2010, Muir et al., 2009, Ster et al., 2009) but in undisturbed lakes were higher in all our study lakes except 14a. Average focus corrected mercury fluxes in both undisturbed lakes (0.253±0.03µg m $^{-2}$ y $^{-1}$) and disturbed lakes (0.266±0.07 µg m $^{-2}$ y $^{-1}$) were similar, however anthropogenic Hg fluxes in sediment profiles increased to the surface in all study lakes except 2a and 9b (ΔHgF_F = -69 - 66 µg m $^{-2}$ y $^{-1}$).

In order to estimate the Hg influx from catchment erosion and permafrost degredation, ΔHgF_F values were adjusted for post-1850 changes in sedimentation rate to obtain $\Delta HgF_{F,adj}$

following the methods of Muir et al., 2009. Average $HgF_{F,adj}$ values (-139-0.03 $\mu g m^{-2} y^{-1}$) were lower than HgF_F values for our study lake indicating the great role of catchment Hg influx.

Similarities between vertical profiles of TOC, S2 carbon, inferred chlorophyll *a* and total Hg were generally apparent within the sediment cores of reference lakes (Figure3.3). For example, Lake 2a showed little fluctuation in these four constituents, whereas Lake 9a and 36a showed surface enrichment in all of them. Lake 14a had moderate surface enrichment of TOC, S2, and inferred chlorophyll *a* and Hg surface enrichment. Similarly, permafrost slump lakes showed less surface enrichment in Hg, TOC, S2, and inferred chlorophyll *a* in Lakes 2b, 9b, and 36b compared to control lakes, whereas 14b showed the lowest surface Hg enrichment (Figure 3.4). Enrichment factors for Hg were 1.16-1.48 and were similar to values reported in other Arctic regions (1.1-2.6, Cooke et al., 2010; Kirk et al., 2011; Muir et al., 2009; Stern et al., 2009).

These results corroborate results in Chapter 2 showing a dilution of sedimentary organic matter by inorganic clastic materials derived from thaw slumps in these lakes affected by thermokarst. S2 concentrations in these lakes were generally similar to those reported in other Arctic sediment cores (0.3-15 mg g^{-1}, Outridge et al., 2007, Stern et al., 2009, Carrie et al., 2010), however Lakes 9a and 14a had 2 to 3 times higher S2 concentrations (41 and 31 mg g^{-1} respectively). It is unlikely that autochthonous organic production is higher in these lakes, given their oligotrophic status. Low inorganic sedimentation rates are a plausible reason for elevated organic matter concentrations (Rowan et al., 1992).

Sedimentation rates were variable in many of these cores and were occasionally seen to spike at intervals, often with a corresponding drop in sedimentary organic content and water

content (Figures 3.3 and 3.4). This might be expected due to a sudden dilution of organic matter from an influx of inorganic sediment (Chapter 2). Examples are seen in cores from reference lakes and thaw slump lakes: Lakes 9a (at 7-12 cm), 36a (5-10 cm), 2b (3-7 cm), 14b (0-1.5 cm), and 36b (5-6 cm). S2 carbon was inversely correlated with ^{210}Pb-derived sedimentation rates (based on the constant rate of supply model) in some of these cores, particularly those where sedimentation rates exceeded 1,000 g m^{-2} y^{-1} (Figure 3.6).

These correlations may have resulted from organic matter dilution during periods of rapid inorganic sedimentation such as those that occur from permafrost thaw slumping (Chapter 2)

3.4.2-Relationship between Hg and S2

Mercury profiles in 6 of the 8 study lakes were highly correlated with S2 (R^2= 0.21- 0.91, $p<0.05$) (Figure 3.7). The association between mercury concentrations in sediment and S2 suggest that factors affecting autochthonous organic delivery to sediments might also affect mercury delivery to sediments. No temporal correlation was found between S2 and mercury for lakes 14a and 14b in sediment profile.

Significant correlations between Hg and S2 in previous studies (Sanei et al., 2006; Outridge et al., 2007; Stern et al.,2009 and there in references) emphasized the role of algal scavenging of mercury. Other studies observed that Hg was only correlated with S2 in a subset of sediment cores, suggesting that algal scavenging may not explain Hg deposition to sediments in most cases (Kirk et al., 2010; Gälman et al., 2008).

Absence of correlation between Hg and S2 may result from the following circumstances:

1- Algal scavenging may not be a driving factor for Hg deposition to sediments
2- S2 is not exclusive to the algal OM fraction but algal OM is known to have higher S2 concentrations than other plant groups (Taylor et al 1998) so S2 may significantly vary due to OM inputs from terrestrial and other aquatic plants

S2 and inferred chlorophyll *a*were significantly correlated in 7 of 8 lakes ($r=0.44-0.94$, $p<0.05$) butno correlation was observed in lake 2a($r=0.47$, $p>0.05$).(Figure S3.4). Hg and inferred chlorophyll *a* were significantly correlated in 5 of 8 lakes ($r=0.72-0.91$, $p<0.005$) and no correlation in other 3 lakes (14a: $r=0.09$, $p>0.05$; 2a: $r=0.18$, $p>0.005$; and 14b $r=0.45$, $p>0.005$) (Figure S3.5). It should be mentioned that pigments such as inferred chlorophyll *a*are susceptible to degradation due to their O-containing functional groups (Hurley and Armstrong, 1990, 1991; Leavitt and Carpenter, 1990) which might affect its distribution in sediment cores.

3.4.3-Van Krevelen diagrams and kerogen types

Average sediment S2 carbon concentration in all 4 undisturbed lakes were higher (13-41 mg HC g^{-1} dw) than their paired disturbed lakes (3-11 mg HC g^{-1} DW) (Figures 3.3 and 3.4) which were similar to those reported in other Arctic sediment cores (0.3-15 mg g^{-1}) while S2 concentrations in lakes 9a(41mg g^{-1}) and 14 A(31 mg g^{-1}) were higher than the highest amount previously reported in other Arctic lake sediments ((Outridge et al., 2007, Stern et al., 2009, Carrie et al., 2010).

Average sediment S2 fluxes were higher in 3 of 4 undisturbed lakes (9a, 14a, 36a)(4471-23500g m^{-2} y^{-1}) compared to their controls (9b, 14b, 36b) (703-8070 g m^{-2} y (Figure 3.6).

Residual Carbon (RC) forms 72 ± 5 % of the sediment TOC in all the undisturbed lakes and 77±6 % in disturbed lakes which is the major portion of the sediment TOC (Figures 3.3 and 3.4). Based on the formula mentioned in Lafargue, 1998 (TOC=PC+RC) the remaining is pyrolyzed carbon (PC) which contains S2, this might be an indication showing that much of the OC in Arctic lake sediments is char, coal, or reworked oxidized organic matter (Carrie et al. 2010, Peters et al., 2005). This is not surprising since primary productivity and terrigenous OC inputs are low and OC recycling is often intensive in Arctic lakes (Kirk et al., 2010).

The ratios of S2 to RC in all eight lakes were almost consistent throughout the core, indicating that S2 was well preserved (Figures 3.3 and 3.4). Meanwhile there were some slight fluctuations in some parts of the sediment cores which might be due to the independent S2 and RC inputs in these lakes such as permafrost thaw slumping events and other catchment related influxes. Likewise, another study (Galman et al., 2008) indicated a 23% loss of carbon within 27 years of deposition which could be another reason for the observed fluctuations for S2:RC in our sediment cores. The hydrogen index (HI) in our study lakes (291±123 mg HC g^{-1} TOC) was higher in 3 of 4 disturbed lakes compared to their reference lakes, lake 14 b which is a very permafrost slump active lake is the only lake with lower HI (186 mg HC g^{-1} TOC) in comparison with its control (448 HC g^{-1} TOC). The oxygen index (OI) in our lakes (216 ± 89 mg CO_2 g^{-1} TOC) was higher in two of the undisturbed lakes than their controls and vice versa in another two pairs (figure 3.8). Our HI and OI values were similar to those reported previously in the region(202 ± 78 mg HC g^{-1} TOC and OI 223 ± 99 mg CO_2 g^{-1} TOC) (Kirk et al., 2010).

Characteristic of type III and type II/type III kerogen mixtures are determined by plotting HI and OI values (Van Krevelen) and S2:TOC diagrams (Figures 3.8 and 3.9).

Organic carbon in our study lakes mainly showed type III (figures 3.8 and 3.9) which originates from terrestrial plants whereas type II kerogen is derived from a mixture of algal, invertebrate, and bacterial debris (Peters et al., 2005) but it also can be as a result of reworked oxidized organic matter including algal derived OC (Carrie et al. 2010, Peters et al., 2005) and intensive OC recycling in Arctic lakes (Kirk et al., 2010).

3.5-Conclusions

Sediment cores from lakes with pronounced thaw slumps were compared with nearby reference lakes to assess the impact of thaw slump development on mercury and organic sedimentation in lakes of the Mackenzie Delta uplands region. The results show that sediments from lakes disturbed by thaw slump development contained lower concentrations of total organic carbon and S2 organic fractions, lower mercury, methyl mercury concentrations as well as higher total and inorganic sedimentation rates. Total Hg concentrations in profile were correlated with total organic carbon (TOC), algal derived (S2) organic carbon, and sediment inferred chlorophyll *a*content in most cores, showing that autochthonous organic carbon production was related to Hg delivery in these sediments. Temporal correlations between mercury and S2 in all our study lakes except one pair (14a and 14b) generally supported the hypothesis that algal derived materials are important sources of Hg to sediments. We observed higher S2 concentrations in reference lakes

than in slump lakes, likely due to lower dilution by flux of inorganic clastic matter. We show that permafrost thaw slump development in the Mackenzie Delta region generally increased sedimentation of inorganic matter in sedimentary archives, diluting organic carbon and Hg in lake sediments.

3.6-Acknowledgments

This study was funded by a Natural Sciences and Engineering Research Council (Canada) Strategic Projects grant to JMB, JPS, and MFJP. Logistical support was provided by the Polar Continental Shelf Program (PCSP). We thank Peter deMontigny for field assistance.

References

Carrie, J.;Wang, F.; Sanei,H.;Macdonald, R.W.;Outridge, P.M.; Stern, G. A.Increasing contaminant burdens in an arctic fish, burbot (Lotalota), in a warming climate. *Environ. Sci. Technol*. 2010, 44, 316–322.

Cooke, C. A.; Hobbs, W.O.Neal, M. Wolfe, A. P., Reliance on ^{210}Pb chronology can compromise the inference of preindustrial hg flux to lake sediments. *Environ. Sci. Technol.* 2010, 44, 1998-2003.

Espitalié J, Laporte J-L, Madec M et al (1977) Méthode rapide de caractéristique des roches mères, de leur potentiel pétrolier et de leur degré d'évolution. Revue de l'Institut français du Pétrole, 32: 23-42.

Gälman, V., Rydberg, J., de-Luna, S.S., Bindler, R.,Renberg, I.Carbon and nitrogenloss rates during aging of lake sediment: Changes over 27 years studied in varved lake sediment. *Limnol.Oceanogr.* 2008,*53*, 1076-1082.

Goodarzi, F., Reyes, J., Schulz, J., Hollman, D., Rose, D., 2006. Parameters influencing the variation in mercury emissions from an Alberta power plant burning high inertinite coal over38 weeks period. Int. J. Coal Geol. 65, 26–34

Hobbie, J.E., Peterson, B.J., Bettez, N., Deegan, L., O'Brien, W.J., Kling, G.W., Kipphut, G.W., Bowden, W.B., et al. 1999. Impact on global change on the biogeochemistry and ecosystems of an arctic freshwater system. *Polar Res*. 18, 207–214.

Jiang, S.; Liu, X.; Chen, Q. Distribution of total mercury and methylmercury in lake sediments inArctic Ny-Alesund. *Chemosphere,*2011, doi:10.1016/j.chemosphere.2011.01.031.

Langford FF, Blanc-Valleron MM (1990) Interpreting Rock-Eval pyrolysis data using graphs of pyrolyzable hydrocarbons vs. total organic carbon. American Association of PetroleumGeology Bulletin 74: 799-804.

Larter SR, Horsfield B (1993) Determination of structural components of kerogens by the use of analyticalpyrolysis. In Organic Geochemistry (Edited by Engel M.H. and Macko S.A.), pp. 271-287. Ch.13, Plenum Press.

Muir,D.C.G.;Wang, X.; Yang, F.;Nguyen,N.; Jackson, T.; Evans, M.;Douglas,M.;Ko ¨ck,G.; Lamoureux, S.; Pienitz,R.; et al. Spatial trends and historical deposition of mercury in eastern and northern Canada inferred from lake sediment cores. *Environ. Sci. Technol.* 2009, 43, 4802–4809.

Macdonald RW, Harner T, Fyfe J. 2005. Recent climate change in the Arctic and its impact on contaminant pathways and interpretation of temporal trend data. *Sci. Tot. Environ*. 342: 5-86.

Macdonald RW and Loseto LL, 2010. Are Arctic Ocean ecosystems exceptionally vulnerable to global emissions of mercury? A call for emphasized research on methylation and the consequences of climate change. *Environmental Chemistry*, 7: 133-138.

McGuire AD, Macdonald RW, Schuur EAG, Harden JW, Hayes DJ, Christensen TR and Heimann M. 2010. The carbon budget of the northern cryosphere region Current Opinion in Environmental Sustainability in press.

Michelutti, N.; Wolfe, A.P.; Vinebrooke, R.D.; Rivard, B.; Briner, J.P. Recent primary production increases in arctic lakes. *Geophys. Res. Lett*. 2005**,** *32*, L19715, doi:10.1029/2005GL023693.

Outridge PM, Sanei H, Stern GA, Hamilton PB, Goodarzi F. 2007. Evidence for control of mercury accucmulation rates in Canadain High Arctic lake sediments by variations of aqatic primary productivity. *Environ. Sci. Technol*. 41: 5259-5265.

Pavlov AV. 1994. Current changes of climate and permafrost in the Arctic and Sub-Arctic of Russia. *Permafrost Periglac*. Process. 5: 101-110.

Pickhardt PC, Folt CL, Chen CY, Klaue B, Blum, JD. 2002. Algal blooms reduce uptake of toxic methylmercury in freshwater food webs. *Proceedings of the National Academy of Sciences* 99: 4419-4423.

Prowse TD, Wrona FJ, Reist JD, Gibson JJ, Hobbie JE, Lévesque LMJ, and Vincent WF. 2006. Climate change effects on hydroecology of Arctic freshwater ecosystems. *Ambio* 35: 347-358.

Peters, K.E.,Walters, C.C.,Moldowan, J.M., 2005. The Biomarker Guide. Vol. 1. *Cambridge University Press*, New York. 471 p.

Reuss, N.; Leavitt, P.R.; Hall, R.I.; Bigler, C.; Hammarlund, D. Development and application of sedimentary pigments for assessing effects of climatic and environmental changes on subarctic lakes in northern Sweden. *J. Paleolimnol*. 2010,*43*, 149-169.

Rowan, D. J., J. Kalff, and J. B. Rasmussen. 1992a. Estimatingthe mud deposition boundary

depth in lakes from wave theory.*Can. J. Fish. Aquat. Sci*. 45: 1436–1447.

Stern, G. A.; Sanei, H.; Roach, P.; De La Ronde, J.; Outridge, P. M. Historical interrelated variations of mercury and aquatic organic matter in lake sediment cores from a subarctic lake in Yukon, Canada: Further evidence toward the algal-mercury scavenging hypothesis. *Environ. Sci. Technol*. 2009, 43, 7684–7690.

Sanei H, Stasiuk LD, Goodarzi F. 2005. Petrological changes occurring in organic matter from recent lacustrine sediments during thermal alteration by Rock-Eval pyrolysis. *Org. Geochem*. 36: 1190–1203.

Serreze MC, Walsh JE, Chapin III FS, Osterkamp T, Dyurgerov M, Ramanovsky V, Oechel WC, Morison J, Zhang T, and Barry RG. 2000. Observational evidence of recent change in the northern high-latitude environment. *Climatic Change* 46: 159-207.

Smol JP, Douglas MSV. 2007. Crossing the final ecological threshold in high Arctic ponds. *Proc. Nat. Acad. Sci*. 104: 12395-12397.

Stern GA, Braekevelt E, Helm PA, Bidleman TF, Outridge PM, Lockhart WL, McNeely R, Rosenberg B, Ikonomou MG, Hamilton MG, Tomy GT, Wilkinson P. 2005. Modern and historical fluxes of halogenated organic contaminants to a lake in the Canadian Arctic, as determined from annually laminated sediment cores. *Sci. Tot. Environ*. 342: 223-243.

St Louis VL, Rudd JWM, Kelly CA, Bodaly RA, Paterson MJ, Beaty KG, Hesslein RH, Heyes A, Majewski AR. 2004. The rise and fall of mercury methylation in an experimental reservoir. *Environ. Sci. Technol.* 38: 1348-1358.

Stern, G.A.; Sanei, H.; Roach, P.; Delaronde, J.; Outridge, P.M. Historical interrelated variations of mercury and aquatic organic matter in lake sediment cores from a subarctic lake in Yukon, Canada: further evidence toward the algal-mercury scavenging hypothesis. *Environ. Sci. Technol*. 2009 *43*, 7684–7690.

Sanei, H.; Outridge, P.M.; Dallimore, A.; Hamilton, P.B. Mercury–organic matter relationships in pre-pollution sediments of thermokarst lakes from the Mackenzie River Delta, Canada: the role of depositional environment. *Biogeochem.* 2010,doi: 10.1007/s10533-010-9543-1.

Stern, G. A.; Sanei, H.; Roach, P.; De La Ronde, J.; Outridge, P. M. Historical interrelated variations of mercury and aquatic organic matter in lake sediment cores from a subarctic lake in Yukon, Canada: Further evidence toward the algal-mercury scavenging hypothesis. *Environ. Sci. Technol*. 2009, 43, 7684-7690.

Tissot B, Durand B, Espitalié J et al (1974) Influence of the nature and diagenesis of organic matter in the formation of petroleum. *AmerAssoc Petrol Geol* Bull 58: 499-506.

Van Krevelen DW (1961) Coal. Typology, chemistry, physics, constitution. Elsevier, New York.

Table 3.1: Location and physical characteristics of the 8 study lakes (4 undisturbed lakes identified by letter a and 4 disturbed by permafrost thaw slump identified by letter b) located in the uplands directly to the east of the Mackenzie River Delta NWT, Canada. Morphometric data and slump activity were determined from air photo analyses and ground surveys undertaken during 2001−2005 (Kokelj et al. 2005).

Lake	Latitude (°N)	Longitude (°W)	Ao[1] (ha)	CA[2] (ha)	SA[3] (ha)	Slump Status	Zm[4] (m)	Ave. FC Sed. Rate g m^{-2} y^{-1}
	Undisturbed Lakes							
2a	68° 50'26.7"	133° 66' 07.1"	2	17.2	–	–	6.1	436
9a	68° 58' 05.8"	133° 53' 53.0"	3.1	29.3	–	–	2.7	475
14a	68° 31' 02.7"	133° 44' 55.4"	3.4	33.5	–	–	7.5	150
36a	68° 30' 10.4"	133° 42' 02.2"	0.8	6.6	–	–	9.5	758
	Disturbed Lakes							
2b	68° 50' 72.8"	133° 67' 03.6"	4.9	15.9	0.95	Stable	3.4	1745
9b	68° 58' 14.1"	133° 53' 59.3"	3.6	7.2	2.5	Active	3	868
14b	68° 31' 02.7"	133° 44' 55.4"	9.2	45.1	2.4	Active	10.5	858
36b	68° 30' 09.6"	133° 42' 05.2"	3.9	24.4	4.9	Stable	7.4	281

[1]$A_{o=}$ lake surface area

[2]CA= catchment area

[3]SA= area of retrogressive thaw slump

[4]$Z_{m=}$ maximum depth of lake

[5]Average sedimentation rate (focus corrected to 50 Bq m^{-2} y^{-1}) using the CFCS model

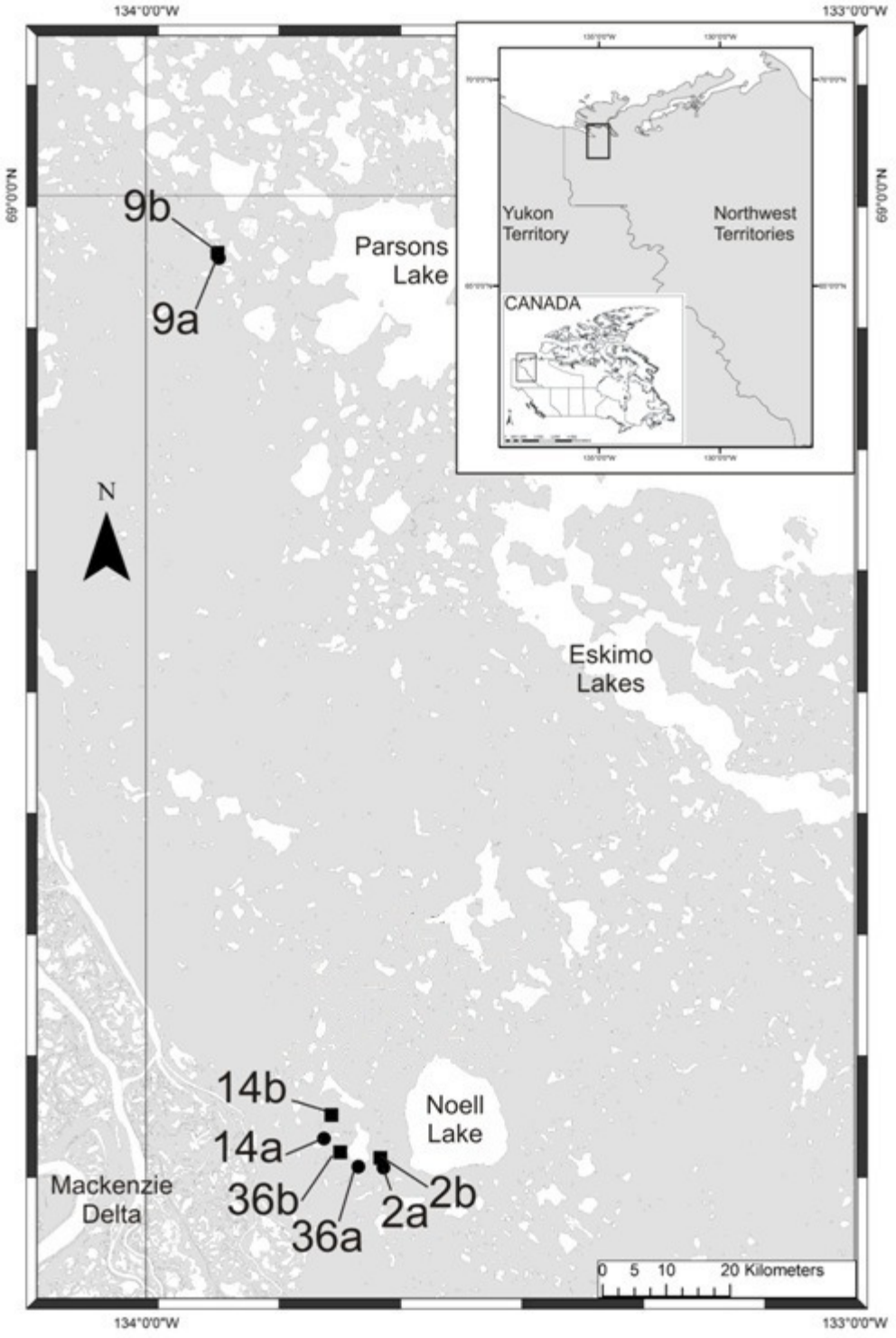

Figure 3.1: Map of study lakes in the Mackenzie Delta near Inuvik. Lakes denoted 'a' are undisturbed lakes, and those denoted 'b' have catchments disturbed by permafrost melting.

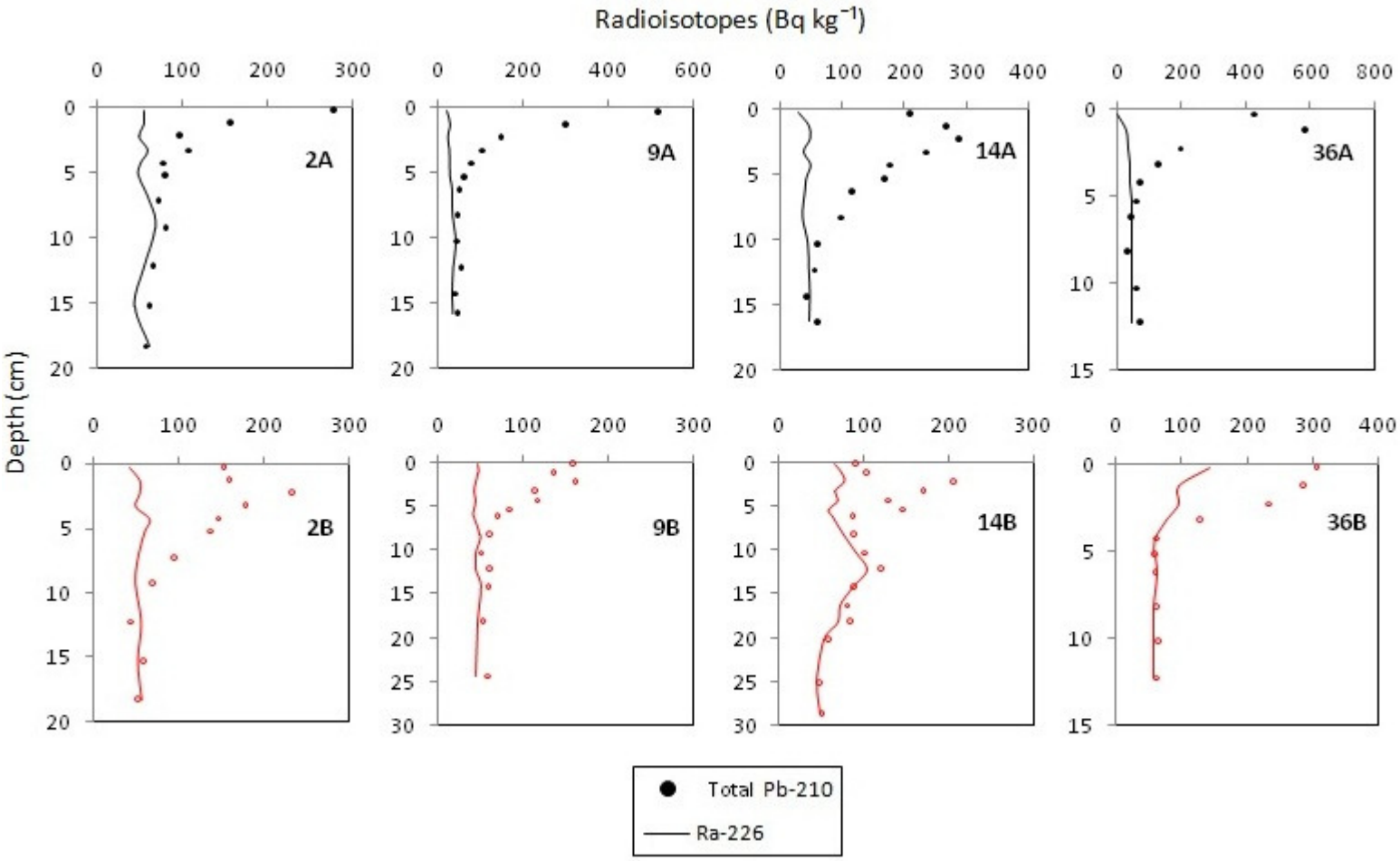

Figure 3.2: Total ^{210}Pb and ^{226}Ra (Bq kg^{-1}) versus depth (cm) in 8 study lakes, 4 undisturbed lakes (a) and 4 lakes disturbed by thaw slumps (b) in the Mackenzie Delta.

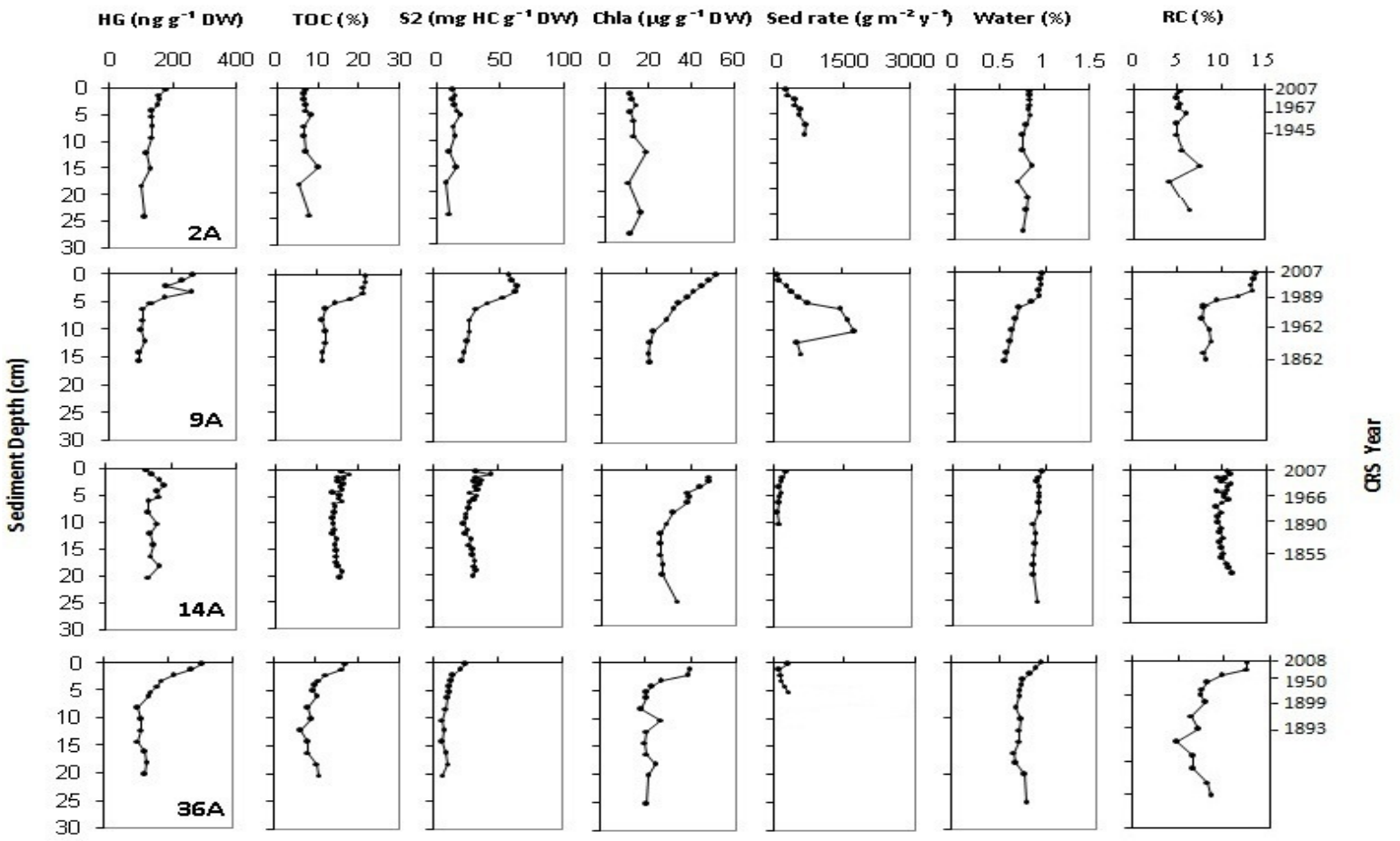

Figure 3.3: The temporal distribution of sediment mercury (ng g^{-1} DW), TOC(%), algal derived (S2) carbon (mg Hc g^{-1} DW), inferred chlorophyll *a* (µg g^{-1} DW), sedimentation rate (focus corrected to 50 Bq m^{-2} y^{-1} excess ^{210}Pb), percent water (%), and RC plotted against sediment cores depth in 4 undisturbed (reference) lakes in the Mackenzie Delta.

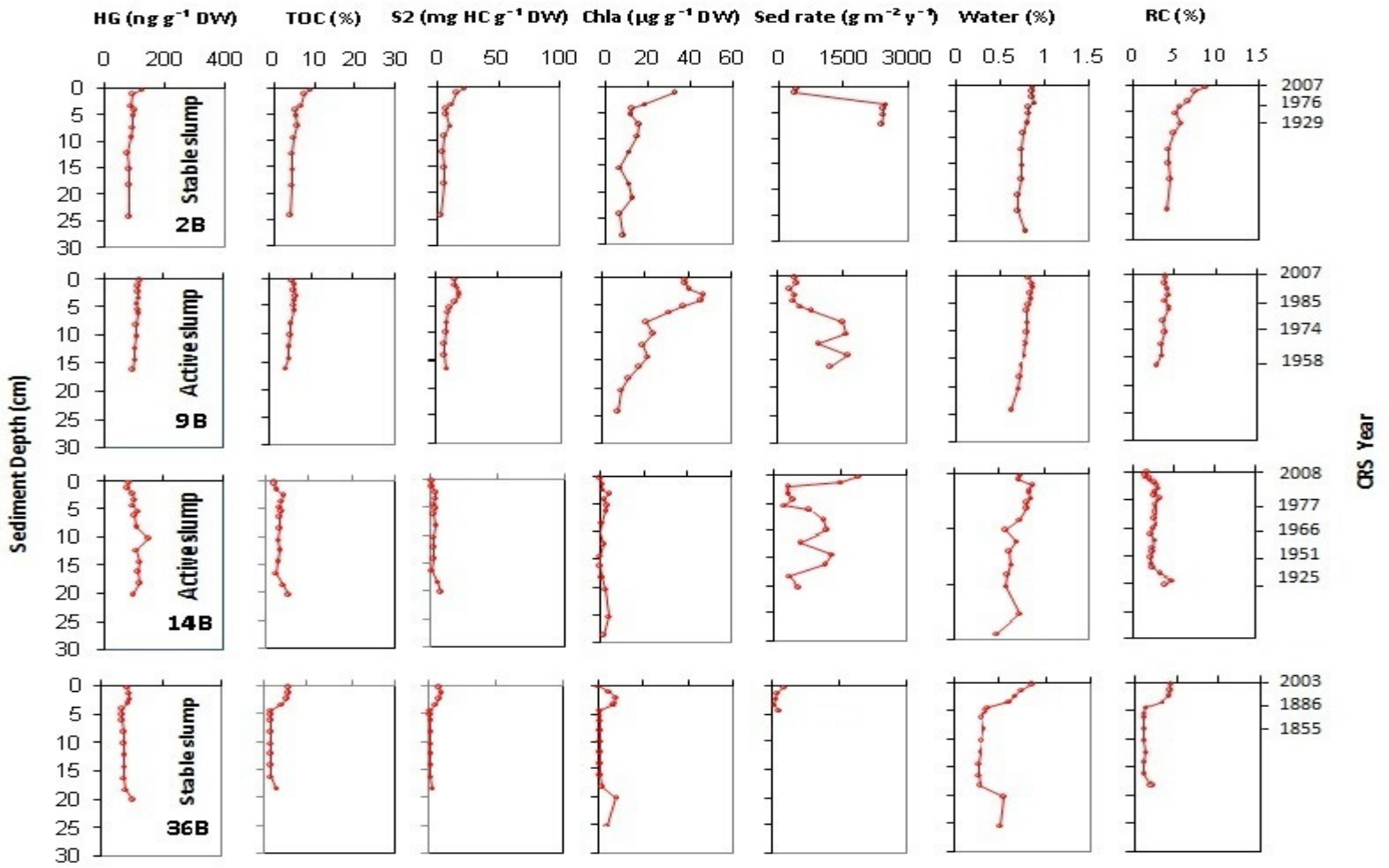

Figure 3.4: The temporal distribution of sediment mercury (ng g^{-1} DW), TOC(%), algal derived (S2) carbon (mg Hc g^{-1} DW), inferred chlorophyll *a* (µg g^{-1} DW), sedimentation rate (focus corrected to 50 Bq m^{-2} y^{-1} excess ^{210}Pb), percent water (%), and RC plotted against sediment cores depth in 4 disturbed (thaw slump) lakes in the Mackenzie Delta.

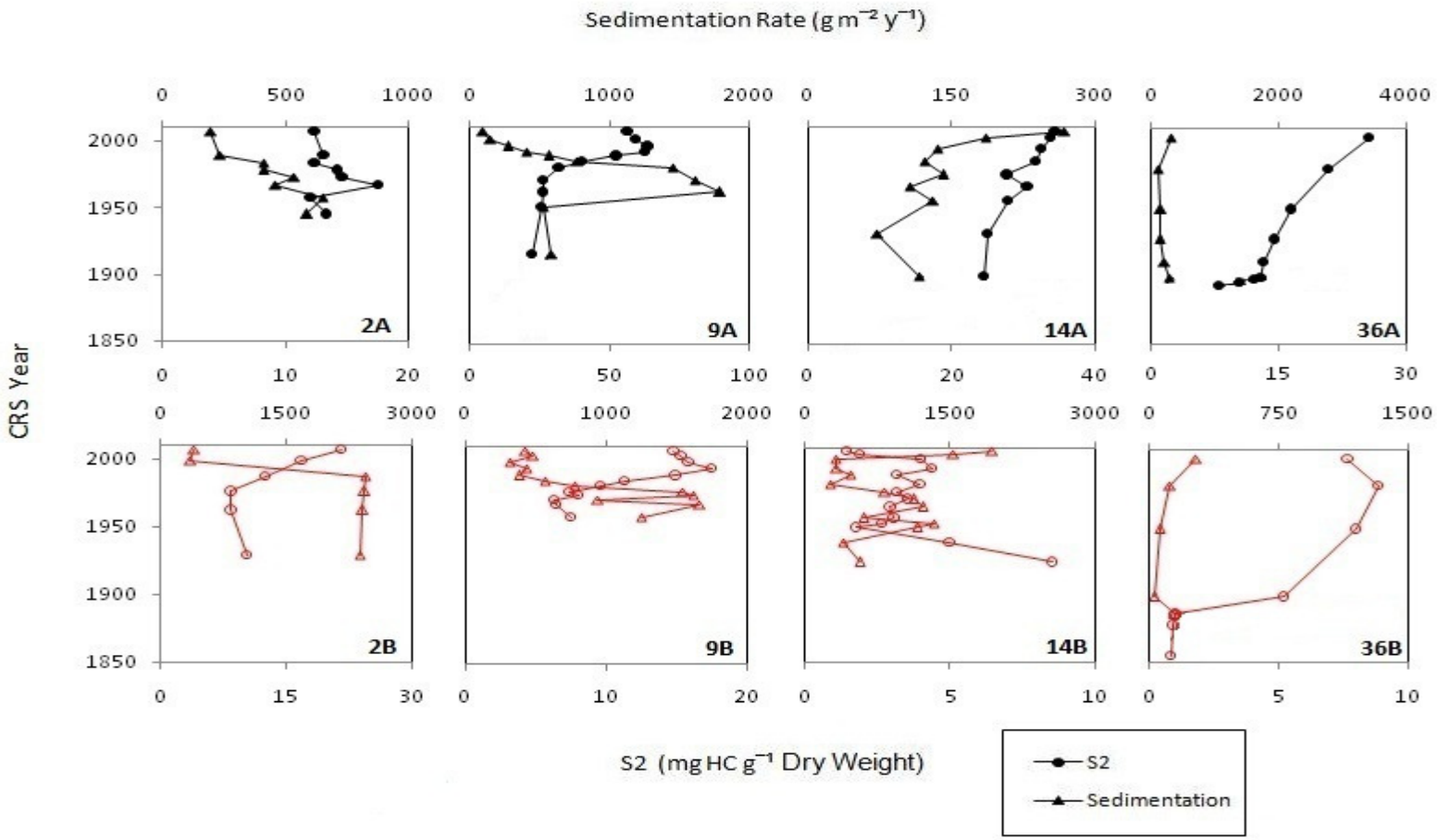

Figure 3.5: Sedimentation rate (g m^{-2} y^{-1}) and algal derived (S2) carbon (mg HC g^{1} DW) through time in 8 lake sediment cores, 4 undisturbed lakes (a) and 4 lakes disturbed by thaw slumps (b) in the Mackenzie Delta.

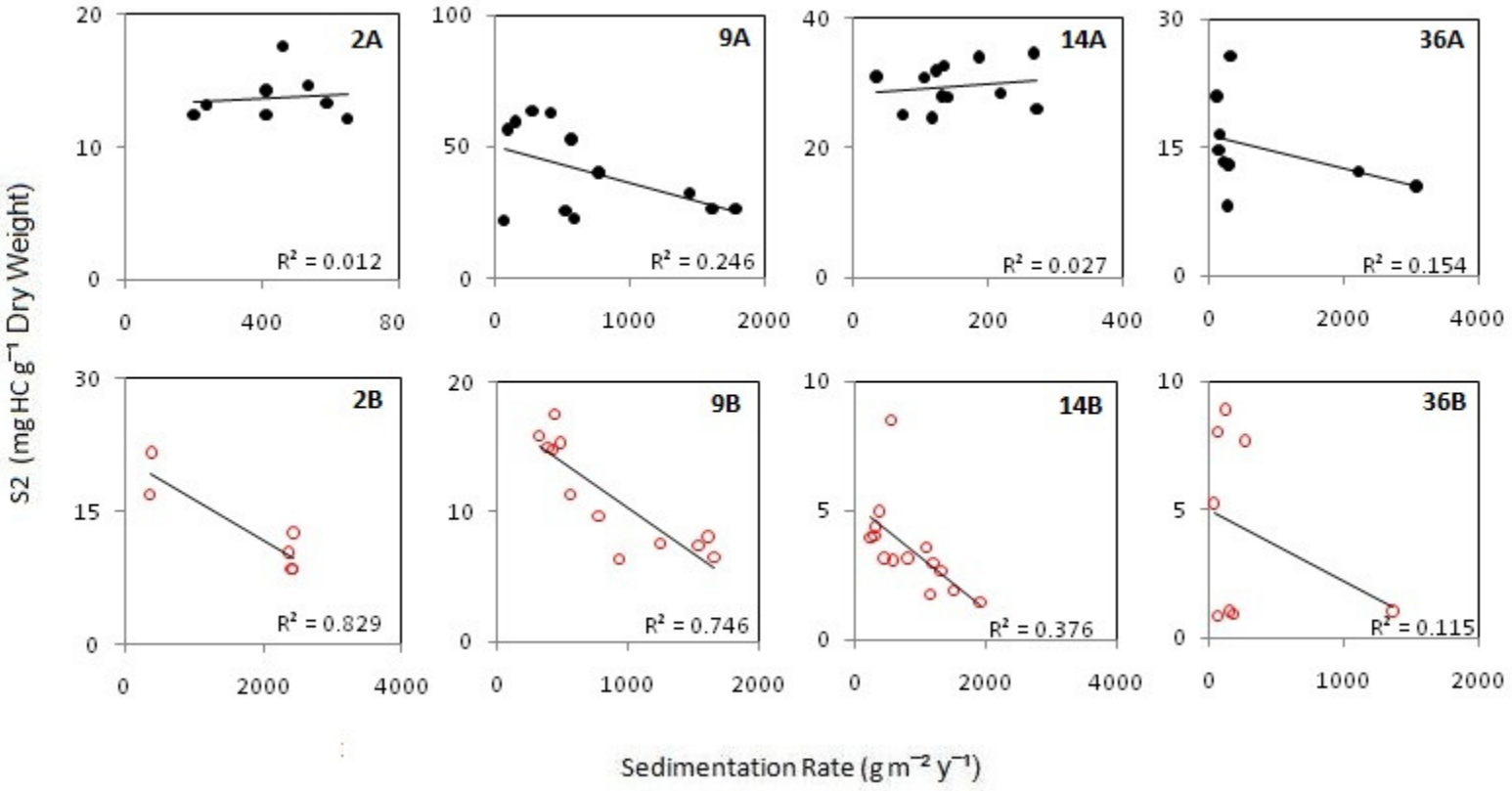

Figure 3.6: Sedimentation rate (g m^{-2} y^{-1}) plotted against algal-derived (S2) organic carbon (mg HC g^{-1} DW) in 8 study lakes, 4 undisturbed lakes (a) and 4 lakes disturbed by thaw slumps (b) in the Mackenzie Delta.

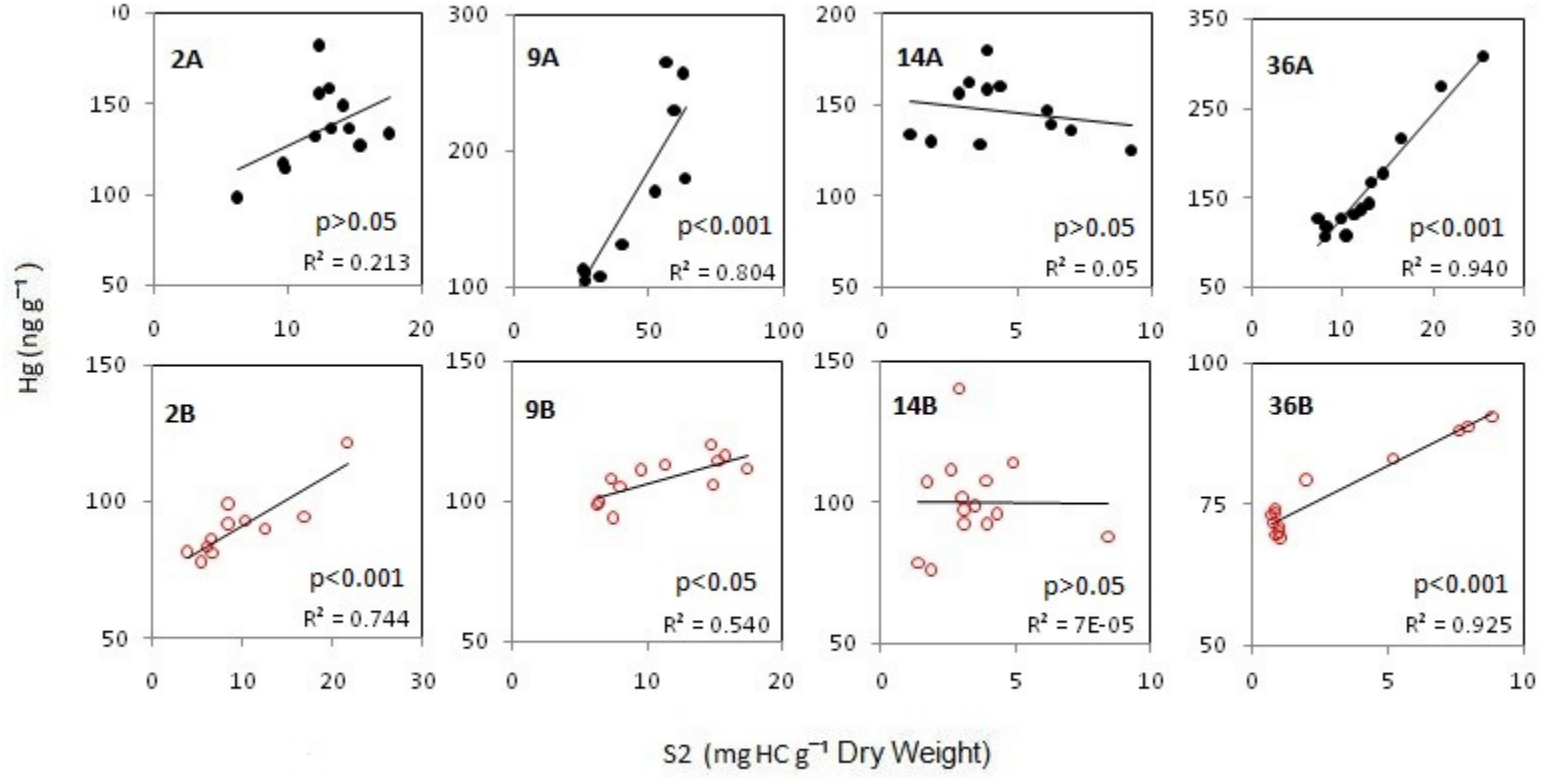

Figure3.7: Hg concentration plotted against algal-derived (S2) organic carbon in 8 study lakes, 4 undisturbed lakes (a) and 4 lakes disturbed by thaw slumps (b) in the Mackenzie Delta.

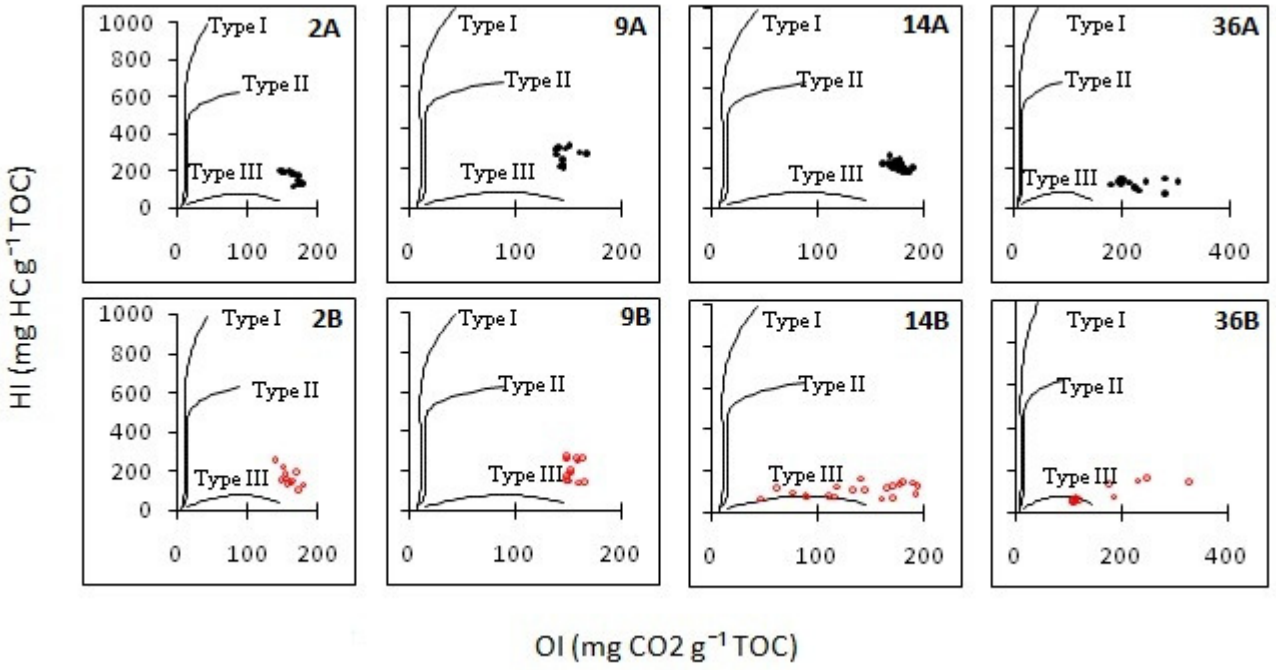

Figure3.8: Van Krevelen diagram showing kerogen type in sediment cores from 8 study lakes, 4 undisturbed lakes (a) and 4 lakes disturbed by thaw slumps (b) in the Mackenzie Delta region as determined by hydrogen index (HI) and oxygen index (OI). The solid curves define the boundaries of Type I, II, and III kerogens (Peters et al., 2005 and references therein).

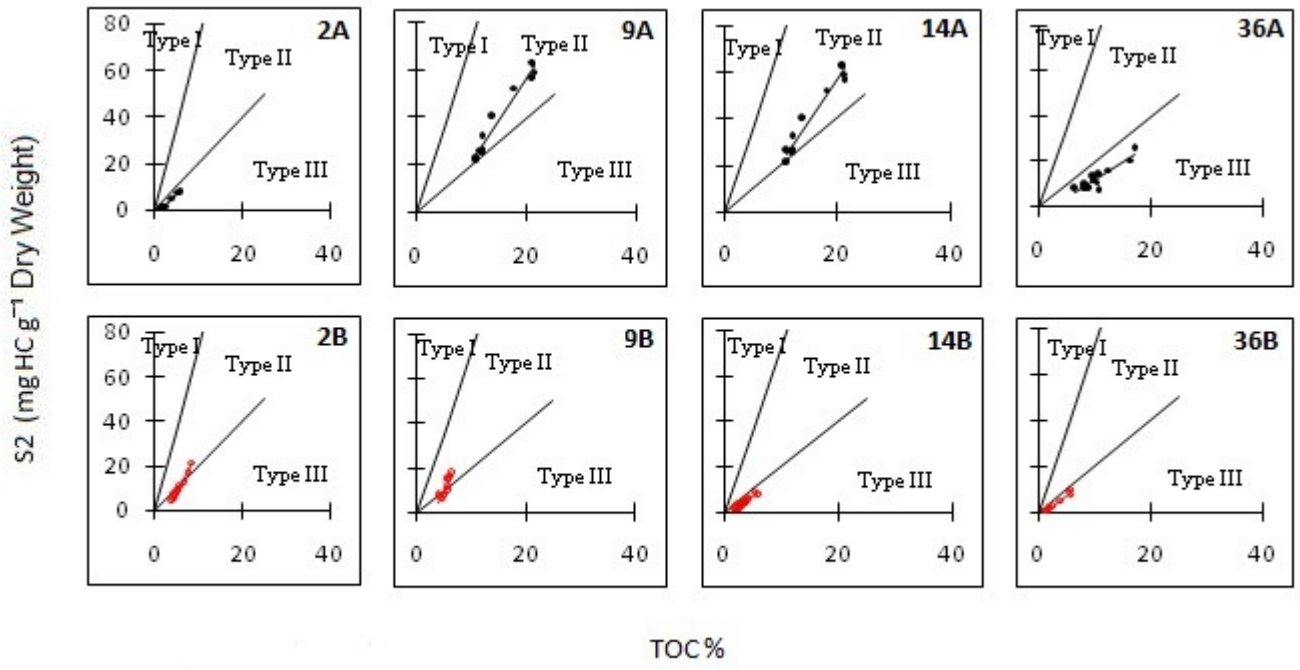

Figure 3.9: Kerogen type in sediment cores from 8 study lakes, 4 undisturbed lakes (a) and 4 lakes disturbed by thaw slumps (b) in the Mackenzie Delta region as determined by S2 and TOC. The solid curves define the boundaries of Type I, II, and III kerogens (Peters et al., 2005 and references therein).

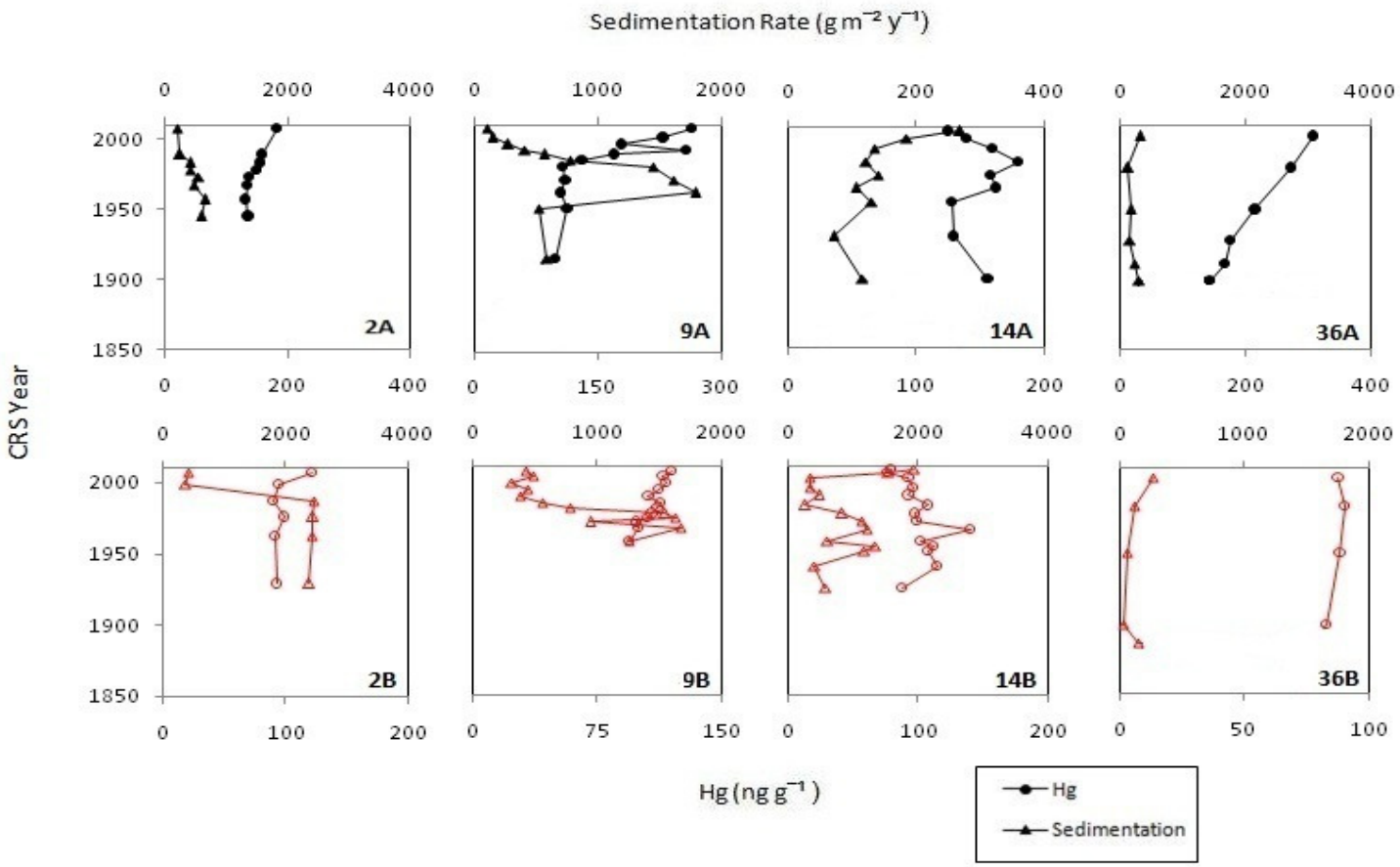

Supplemental Figure (Figure S3.1) (Appendix): Sedimentation rate (g m^{-2} y^{-1}) and Hg concentration (ng g^{-1}) in dated horizons of sediment cores from 8 study lakes, 4 undisturbed lakes (a) and 4 lakes disturbed by thaw slumps (b) in the Mackenzie Delta region.

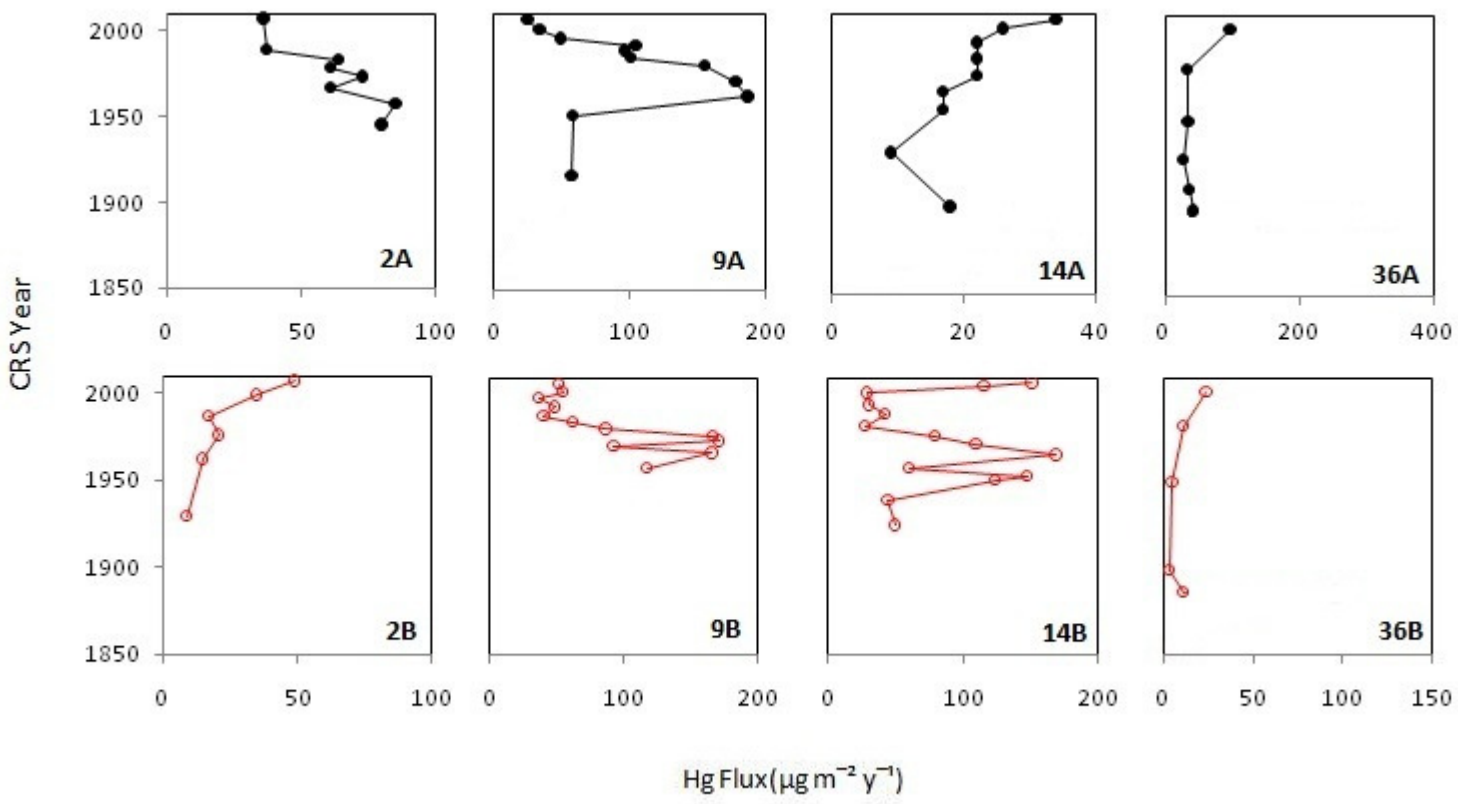

Supplemental Figure (Figure S3.2) (Appendix): Mercury flux (µ m^{-2} y^{-1}) through time in 8 study lakes, 4 undisturbed lakes (a) and 4 lakes disturbed by thaw slumps (b) in the Mackenzie Delta.

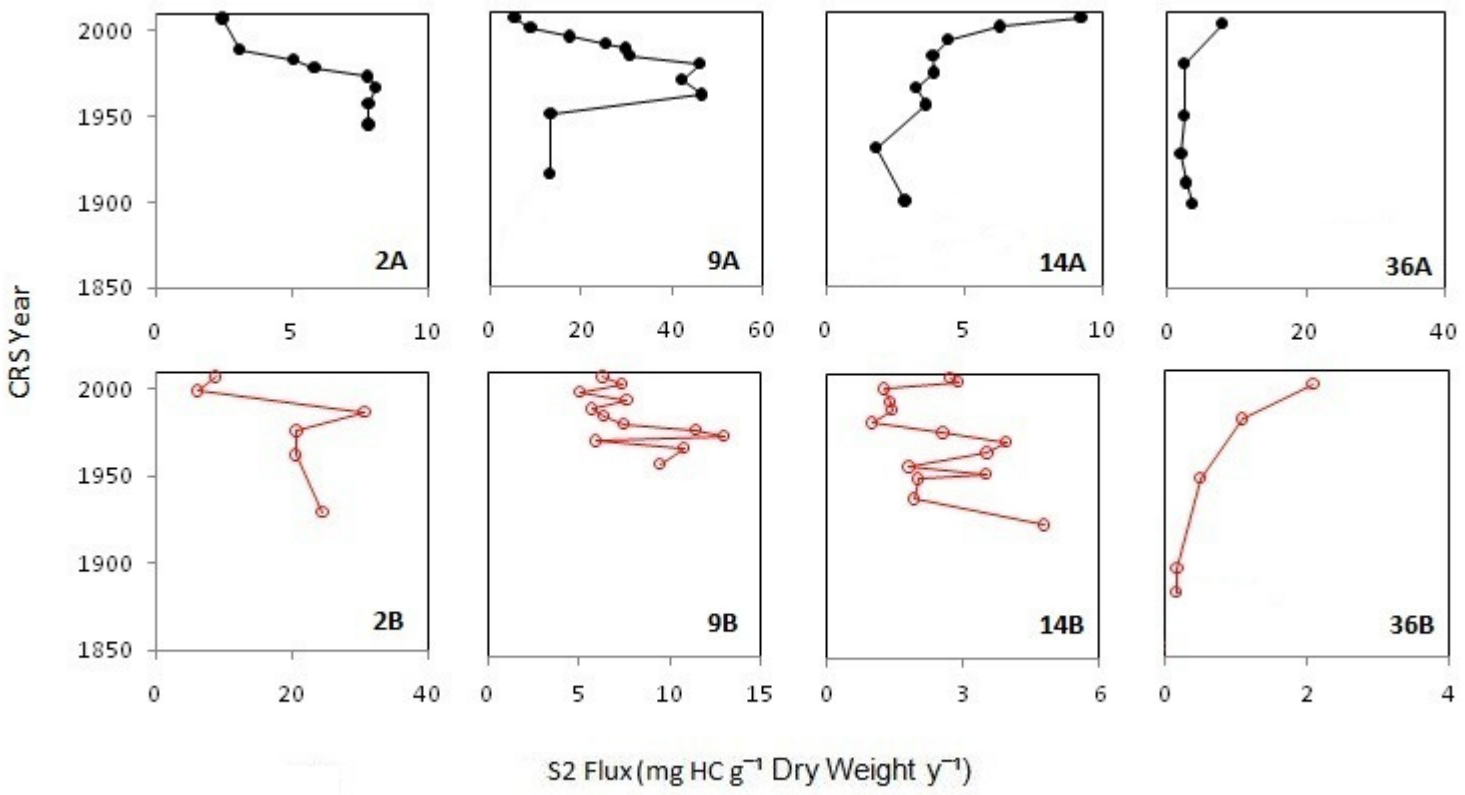

Supplemental Figure(Figure S3.3) (Appendix). Algal derived (S2) carbon flux (mg HC g^{-1} DW y^{-1}) in dated horizons from 8 study lakes, 4 undisturbed lakes (a) and 4 lakes disturbed by thaw slumps (b) in the Mackenzie Delta.

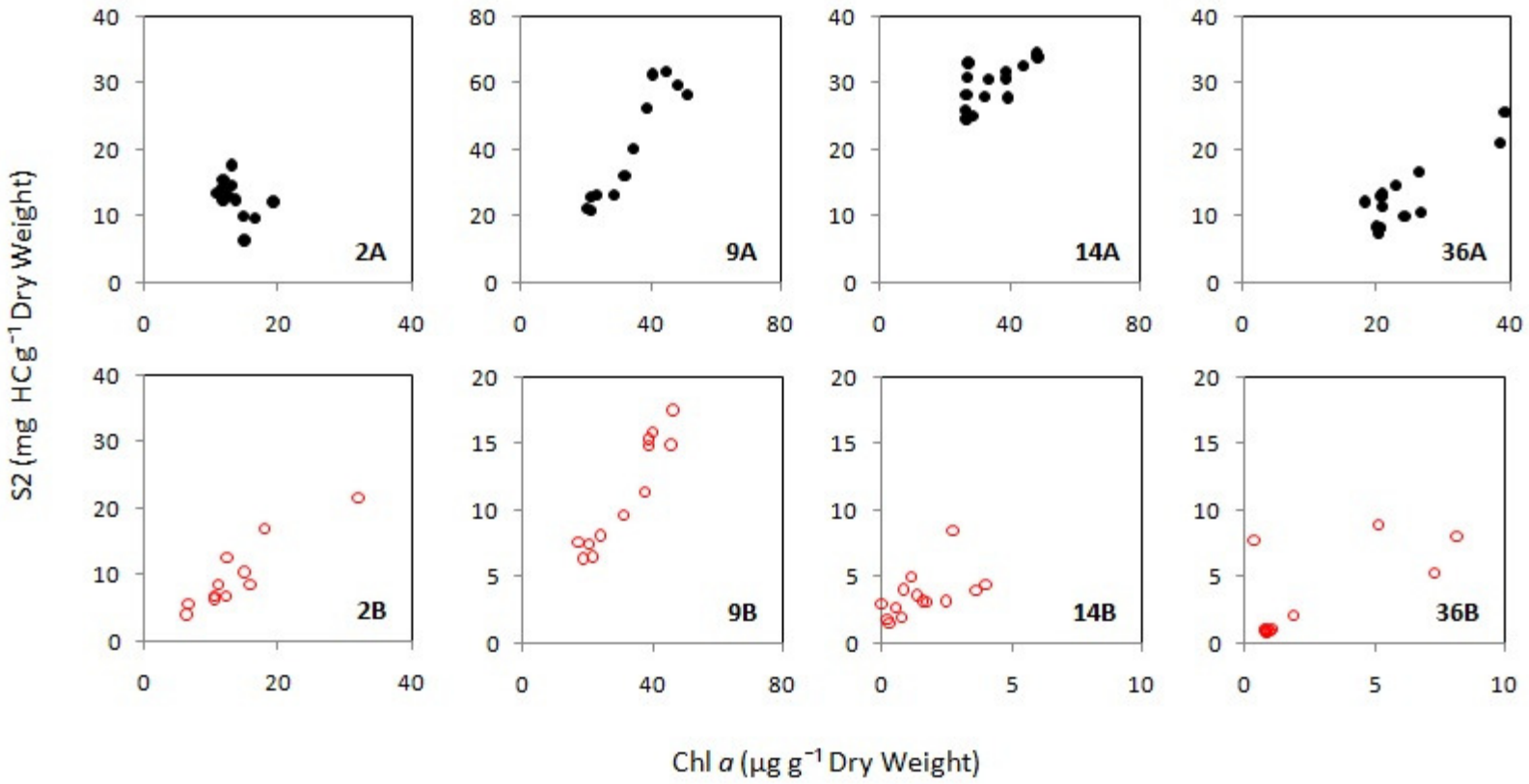

Supplemental Figure(Figure S3.4) (Appendix). Algal derived (S2) carbon (mg HC g^{-1} DW) plotted against inferred chlorophyll *a*(µg g^{-1} DW) in 8 study lakes, 4 undisturbed lakes (a) and 4 lakes disturbed by thaw slumps (b) in the Mackenzie Delta.

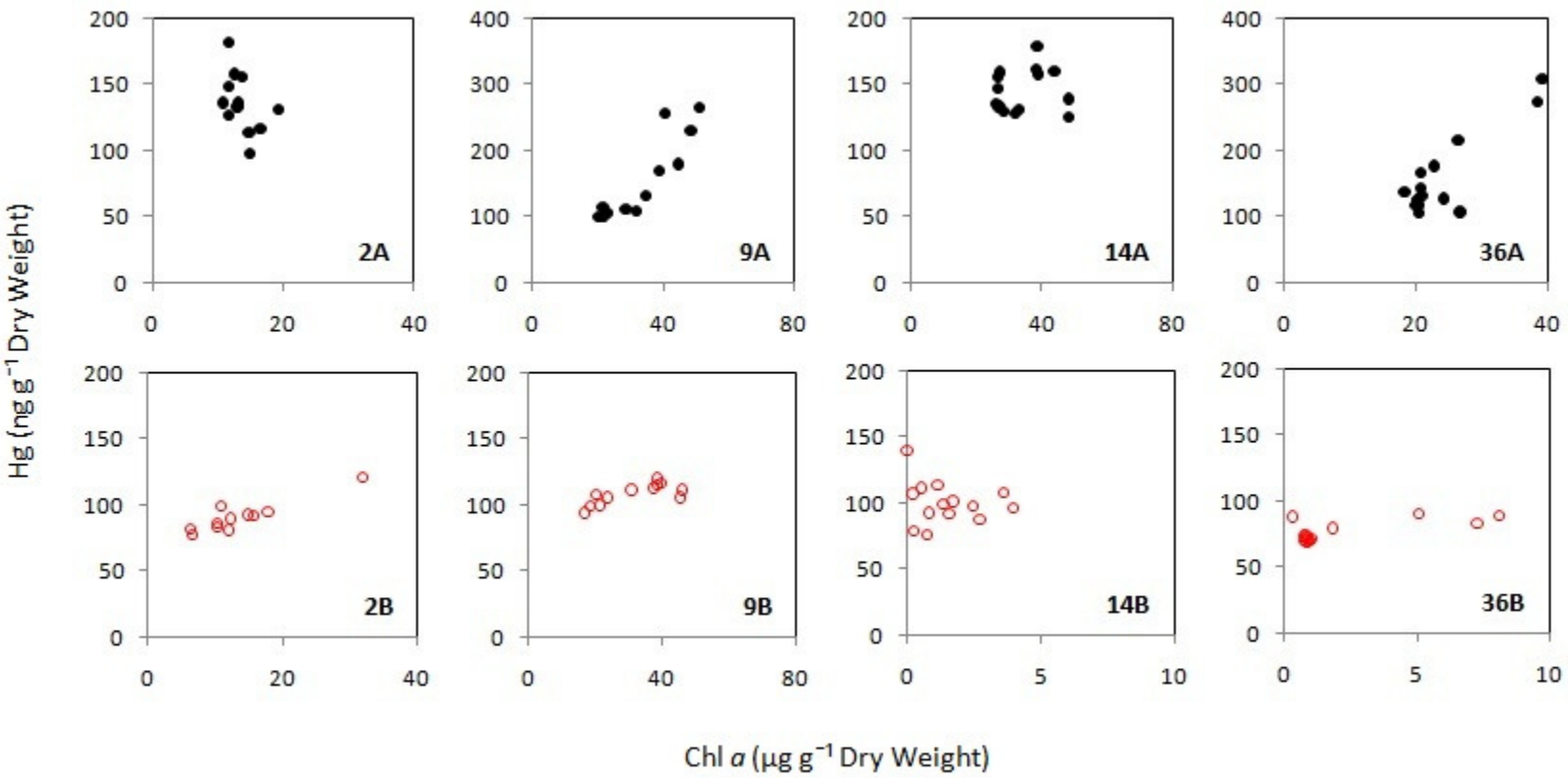

Supplemental Figure (Figure S3.5) (Appendix). Hg concentration (ng g^{-1} DW) and inferred chlorophyll *a*(µg g^{-1} DW) in 8 study lakes, 4 undisturbed lakes (a) and 4 lakes disturbed by thaw slumps (b) in the Mackenzie Delta.

4.0- General Conclusion

In our study we used a paired, comparative analysis of lakes where retrogressive thaw slumps were present (disturbed) and absent (reference).Radiometrically dated sediment cores from thermokarst lakes in the Mackenzie Delta uplands were examined for spatial and temporal analyses to determine how retrogressive thaw slump development from degrading permafrost affected the delivery of mercury (Hg), methylmercury (MeHg) and organic carbon (OC) to lake sediments in thermokarst regions.The results show that sediments from lakes disturbed by thaw slump development contained lower concentrations of total organic carbon and algal derived organic carbon (S2), lower mercury and methyl mercury concentrations, as well as higher total and inorganic sedimentation rates, which likely explain the dilution of organic materials and mercury in lakes where thaw slumps are present. Also,THg concentrations in profile were correlated with total organic carbon (TOC), sediment inferred chlorophyll *a*content, and algal derived (S2) organic carbon in most cores, showing that autochthonous organic carbon production was related to Hg delivery in these sediments with the latter generally supporting the hypothesis that algal-derived materials may be sources of Hg to sediments.

APPENDIX A

Rock-Eval Analyses in Sediment profiles

Table A.1: Rock-Eval analyses for sediment profiles for lake 2a.

Depth (cm)	S1	S2	S3	TOC	RC%	HI	OI	MINC%
0.25	2.86	12.37	12.48	7.21	5.40	172	173	0.7
1.25	3.08	13.13	10.34	6.72	4.90	195	154	0.5
2.25	1.91	12.37	11.26	6.69	5.00	185	168	0.6
3.25	2.14	14.21	12.09	7.29	5.39	195	166	0.6
4.25	2.09	14.59	11.24	7.11	5.22	205	158	0.6
5.25	5.69	17.57	12.61	8.45	5.95	208	149	0.7
7.25	2.60	12.06	10.83	6.74	5.02	179	161	0.7
9.25	3.42	13.31	10.45	6.87	5.01	194	152	0.5
12.25	2.22	9.64	12.62	7.29	5.68	132	173	0.7
15.25	5.58	15.47	17.72	10.18	7.62	152	174	1.0
18.25	1.49	6.27	8.56	5.22	4.18	120	164	0.6
24.25	2.09	9.82	14.31	7.96	6.31	123	180	0.8

Table A.2: Rock-Eval analyses for sediment profiles for lake 2b.

Depth (cm)	S1	S2	S3	TOC	RC%	HI	OI	MINC%
0.25	9.40	21.62	12.04	8.73	5.60	248	138	0.7
1.25	5.41	16.92	11.15	7.44	5.07	227	150	0.6
3.25	4.44	12.55	11.35	6.61	4.67	190	172	0.7
4.25	2.87	8.51	9.03	5.48	4.09	155	165	0.6
5.25	2.51	8.48	7.96	5.10	3.79	166	156	0.6
7.25	2.73	10.31	8.83	5.78	4.27	178	153	0.7
9.25	1.97	6.61	8.74	4.91	3.74	135	178	0.9
12.25	1.33	5.50	6.75	4.36	3.44	126	155	0.5
15.25	1.18	6.22	6.85	4.26	3.30	146	161	0.5
18.25	1.31	6.69	6.62	4.49	3.48	149	147	0.5
24.25	1.05	3.98	6.84	3.95	3.18	101	173	0.5

Table A.3: Rock-Eval analyses for sediment profiles for lake 9a.

Depth (cm)	S1	S2	S3	TOC	RC%	HI	OI	MINC%
0.25	15.70	56.31	35.69	21.25	13.73	265	168	1.3
1.25	16.69	59.35	33.90	21.38	13.55	278	159	1.0
2.25	16.51	63.60	31.62	21.15	13.06	301	150	1.0
3.25	14.44	62.55	30.64	21.02	13.29	298	146	1.1
4.25	10.55	52.51	25.68	18.03	11.67	291	142	1.1
5.25	6.82	40.03	19.17	14.03	9.28	285	137	0.9
6.25	5.94	32.00	16.58	11.95	8.04	268	139	0.6
8.25	5.48	26.32	16.27	11.22	7.81	235	145	0.7
10.25	5.36	26.19	17.36	11.98	8.52	219	145	0.8
12.25	5.14	25.52	17.34	12.12	8.72	211	143	0.8
14.25	4.72	22.29	15.82	11.02	8.01	202	144	0.7
15.75	4.29	21.48	15.92	11.04	8.11	195	144	0.8

Table A.4: Rock-Eval analyses for sediment profiles for lake 9b.

Depth (cm)	S1	S2	S3	TOC	RC%	HI	OI	MINC%
0.25	2.38	14.79	9.34	5.67	3.84	261	165	1.2
1.25	2.69	15.32	9.32	5.85	3.95	262	159	1.1
2.25	2.91	15.86	9.07	6.04	4.08	263	150	0.9
3.25	3.48	17.51	9.81	6.54	4.37	268	150	0.7
4.25	2.81	14.92	9.28	5.86	3.97	255	158	0.8
5.25	3.37	11.35	9.06	5.91	4.26	192	153	0.5
6.25	3.24	9.63	8.63	5.76	4.27	167	150	0.5
8.25	2.60	7.41	7.41	4.98	3.75	149	149	0.5
10.25	2.90	8.05	7.89	5.23	3.90	154	151	0.5
12.25	2.05	6.35	7.58	4.56	3.49	139	166	0.6
14.25	1.79	6.48	7.24	4.50	3.44	144	161	0.5
16.25	0.99	7.55	5.77	3.78	2.81	200	153	0.5

Table A.5: Rock-Eval analyses for sediment profiles for lake 14a.

Depth (cm)	S1	S2	S3	TOC	RC%	HI	OI	MINC%
0.25	14.08	34.46	27.56	15.90	10.59	217	173	1.4
0.75	15.53	44.51	29.24	17.50	11.13	254	167	1.2
1.25	14.82	33.91	26.21	15.12	9.79	224	173	1.2
1.75	13.67	38.44	28.60	16.27	10.58	236	176	1.2
2.25	11.58	32.52	26.53	15.10	10.17	215	176	1.2
2.75	12.02	36.55	28.80	16.39	11.00	223	176	1.2
3.25	10.88	31.80	26.61	15.36	10.61	207	173	1.2
3.75	10.91	35.63	27.61	15.77	10.61	226	175	1.1
4.25	9.44	27.78	24.75	13.73	9.44	202	180	1.1
4.75	11.09	33.13	27.73	15.47	10.48	214	179	1.1
5.25	10.56	30.66	26.57	14.92	10.21	205	178	1.2
5.75	10.74	32.81	28.26	15.83	10.95	207	179	1.3
6.25	9.24	27.84	26.70	14.41	10.05	193	185	1.2
7.25	10.41	28.08	26.77	14.08	9.59	199	190	1.2
8.25	9.35	25.00	26.39	14.33	10.18	174	184	1.3
9.25	9.40	24.91	25.75	13.79	9.69	181	187	1.1
10.25	8.33	24.57	24.67	13.66	9.72	180	181	1.1
11.25	8.29	26.57	25.76	14.18	10.13	187	182	1.1
12.25	7.76	25.86	24.10	13.84	9.95	187	174	1.1
13.25	7.78	28.97	26.09	14.45	10.28	200	181	1.2
14.25	8.41	28.28	25.29	14.09	9.90	201	179	1.1
15.25	9.16	31.40	25.92	14.67	10.08	214	177	1.0
16.25	8.59	30.90	24.56	14.70	10.29	210	167	1.0
17.25	8.66	31.95	25.66	14.60	10.08	219	176	1.0
18.25	7.81	32.98	24.64	15.17	10.65	217	162	1.0
19.25	9.57	34.38	26.49	15.78	10.93	218	168	1.1
20.25	7.90	30.52	26.84	15.72	11.30	194	171	1.1

Table A.6: Rock-Eval analyses for sediment profiles for lake 14b.

Depth (cm)	S1	S2	S3	TOC	RC%	HI	OI	MINC%
0.25	0.13	1.42	3.32	2.07	1.81	69	160	0.2
0.75	0.06	1.26	3.26	1.89	1.65	67	172	0.2
1.25	0.11	1.90	4.26	2.22	1.89	86	192	0.3
1.75	0.35	3.15	8.24	3.12	2.53	101	264	0.4
2.25	0.48	3.99	11.58	3.84	3.04	104	302	0.5
2.75	0.92	5.98	7.80	4.09	3.19	146	191	0.4
3.25	0.51	4.36	6.75	3.48	2.80	125	194	0.4
3.75	0.53	4.04	7.11	3.43	2.77	118	207	0.4
4.25	0.36	3.14	8.82	3.25	2.63	97	271	0.4
4.75	0.81	5.93	7.79	4.27	3.39	139	182	0.4
5.25	0.50	3.96	7.41	3.56	2.89	111	208	0.4
5.75	0.44	3.65	7.69	3.44	2.80	106	224	0.4
6.25	0.34	3.14	8.66	3.34	2.72	94	259	0.4
7.25	0.49	4.39	6.02	3.41	2.76	129	177	0.3
8.25	0.26	3.55	5.20	3.13	2.61	113	166	0.3
9.25	0.28	3.27	4.24	3.17	2.68	103	134	0.3
10.25	0.09	2.93	1.66	2.65	2.30	111	63	0.2
11.25	0.22	1.82	2.77	2.47	2.15	74	112	0.3
12.25	0.24	3.06	4.32	2.95	2.49	104	146	0.3
13.25	0.18	2.13	2.43	2.67	2.36	80	91	0.3
14.25	0.13	2.63	2.09	2.67	2.33	99	78	0.2
15.25	0.12	1.66	1.15	2.40	2.17	69	48	0.2
16.25	0.09	1.75	2.05	2.32	2.06	75	88	0.2
17.25	0.16	2.12	3.19	2.73	2.38	78	117	0.3
18.25	0.34	4.97	4.67	3.94	3.26	126	119	0.4
19.25	1.04	7.45	10.34	6.02	4.83	124	172	0.5
20.25	0.80	8.48	7.29	5.12	4.00	166	142	0.4

Table A.7: Rock-Eval analyses for sediment profiles for lake 36a.

Depth (cm)	S1	S2	S3	TOC	RC%	HI	OI	MINC%
0.25	6.75	25.64	48.08	17.11	12.43	150	281	1.7
1.25	5.52	20.90	40.02	16.47	12.53	127	243	1.7
2.25	4.06	16.50	26.87	12.56	9.67	131	214	1.3
3.25	3.42	14.60	21.83	10.78	8.28	135	203	1.1
4.25	2.49	13.24	19.74	9.85	7.65	134	200	0.9
5.25	2.77	12.94	18.62	9.55	7.38	135	195	0.9
6.25	2.25	12.12	18.41	10.14	8.07	120	182	1.9
8.25	1.90	10.43	15.76	8.24	6.47	127	191	0.9
10.25	1.73	8.09	20.95	9.01	7.22	90	233	1.1
12.25	1.57	8.33	19.93	6.61	4.88	126	302	1.0
14.25	1.36	8.17	18.80	8.34	6.71	98	225	0.9
16.25	1.44	9.88	16.65	8.35	6.66	118	199	0.8
18.25	2.03	11.32	22.70	10.32	8.17	110	220	1.1
20.25	1.72	7.31	29.76	10.58	8.54	69	281	1.4

Table A.8: Rock-Eval analyses for sediment profiles for lake 36b.

Depth (cm)	S1	S2	S3	TOC	RC%	HI	OI	MINC%
0.25	0.69	7.67	18.52	5.59	4.22	137	331	1.0
1.25	1.17	8.87	14.28	5.67	4.29	156	252	0.8
2.25	1.08	7.98	12.12	5.26	4.04	152	230	0.6
3.25	0.66	5.23	7.38	4.09	3.28	128	180	0.4
4.25	0.05	1.04	1.94	1.73	1.56	60	112	0.3
5.25	0.05	1.03	1.87	1.66	1.50	62	113	0.3
6.25	0.04	0.91	1.77	1.60	1.45	57	111	0.3
8.25	0.04	0.86	1.91	1.57	1.41	55	122	0.3
10.25	0.03	0.86	1.81	1.63	1.48	53	111	0.3
12.25	0.04	1.01	1.89	1.68	1.52	60	113	0.3
14.25	0.03	0.78	1.76	1.60	1.46	49	110	0.3
16.25	0.03	0.73	1.73	1.56	1.43	47	111	0.3
18.25	0.15	2.01	4.84	2.61	2.23	77	185	0.3

Table A.9: Rock-Eval analyses for surface sediments for 14 study lakes.

Lake	Depth (cm)	S1	S2	S3	TOC	RC%	HI	OI	MINC%
2a	0.25	2.86	12.37	12.48	7.21	5.4	172	173	0.7
9a	0.25	15.7	56.31	35.69	21.25	13.73	265	168	1.3
14a	0.25	14.08	34.46	27.56	15.9	10.59	217	173	1.4
36a	0.25	6.75	25.64	48.08	17.11	12.43	150	281	1.7
5a	0.25	1.2	7.41	20.21	6.4	5	116	504	0.72
6a	0.25	5.7	22.32	23.62	11.64	8.44	192	325	0.81
7a	0.25	6.41	28.91	33.75	15.15	11.01	191	340	1
2b	0.25	9.4	21.62	12.04	8.73	5.6	248	138	0.7
9b	0.25	2.38	14.79	9.34	5.67	3.84	261	165	1.2
14b	0.25	0.13	1.42	3.32	2.07	1.81	69	160	0.2
36b	0.25	0.69	7.67	18.52	5.59	4.22	137	331	1
5b	0.25	2.81	8.59	10.44	4.69	3.39	183	427	0.57
6b	0.25	10.71	21.49	21.15	11.78	8.29	182	292	0.76
7b	0.25	0.7	5.75	21.94	4.89	3.65	118	695	0.77

APPENDIX B

Mercury Analyses in Sediment profiles

Table B.1: Mercury analyses for sediment profiles for lake 2a.

Depth (cm)	Focus corr sed rate(g m^{-2} y^{-1})	Hg Sed. Rate (µg m^{-2} y^{-1})	Hg (ng g^{-1} DW)
0.25	199	**36**	181.74
1.25	235	37	157.97
2.25	412	64	155.31
3.25	412	61	148.75
4.25	535	73	136.16
5.25	460	61	133.15
7.25	650	85	131.25
9.25	588	80	135.80
12.25			116.68
15.25			126.57
18.25			97.83
24.25			113.73

Table B.2: Mercury analyses for sediment profiles for lake 2b.

Depth (cm)	Focus corr sed rate (g m^{-2} y^{-1})	Hg Sed Rate (µg m-2 y^{-1})	Hg (ng g^{-1} DW)
0.25	405	49	121.14
1.25	367	35	94.27
3.25	2453	17	89.49
4.25	2440	21	98.72
5.25	2422	15	91.53
7.25	2381	9	92.60
9.25			85.79
12.25			77.48
15.25			82.98
18.25			80.90
24.25			81.28

Table B.3: Mercury analyses for sediment profiles for lake 9a.

Depth (cm)	Focus corr sed rate (g m^{-2} y^{-1})	Hg Sed Rate (µg m^{-2} y^{-1})	Hg (ng g^{-1} DW)
0.25	99	26	264.53
1.25	151	35	228.96
2.25	277	50	179.21
3.25	411	105	256.53
4.25	570	97	169.58
5.25	773	101	130.78
6.25	1450	155	107.12
8.25	1612	178	110.44
10.25	1789	187	104.80
12.25	525	59	112.64
14.25	587	58	99.04
15.75	62	6	98.29

Table B.4: Mercury analyses for sediment profiles for lake 9b.

Depth (cm)	Focus corr sed rate(g m^{-2} y^{-1})	Hg Sed Rate (µg m^{-2} y^{-1})	Hg (ng g^{-1} DW)
0.25	430	52	119.908
1.25	482	55	114.493
2.25	318	37	116.169
3.25	438	49	111.5
4.25	387	41	105.625
5.25	563	63	112.667
6.25	780	87	111.132
8.25	1544	167	107.913
10.25	1621	171	105.226
12.25	940	93	98.769
14.25	1666	166	99.679
16.25	1253	118	94.017

Table B.5: Mercury analyses for sediment profiles for lake 14a.

Depth (cm)	Focus corr sed rate(g m^{-2} y^{-1})	Hg Sed Rate (µg m^{-2} y^{-1})	Hg (ng g^{-1} DW)
0.25	269	34	124.866
0.75			
1.25	186	26	139.087
1.75			
2.25	135	22	159.544
2.75			
3.25	122	22	179.288
3.75			
4.25	141	22	157.849
4.75			
5.25	106	17	161.804
5.75			
6.25	131	17	127.581
7.25			
8.25	73	9	129.414
9.25			
10.25	117	18	155.64
11.25			
12.25	272	32	135.512
13.25			
14.25	218	37	146.809
15.25			
16.25	34	5	132.988
17.25			
18.25			159.474
19.25			
20.25			131.02

Table B.6: Mercury analyses for sediment profiles for lake 14b.

Depth (cm)	Focus corr sed rate($g\ m^{-2}\ y^{-1}$)	Hg Sed Rate ($\mu g\ m^{-2} y^{-1}$)	Hg ($ng\ g^{-1}$ DW)
0.25	1928	151	78.285
0.75			
1.25	1531	116	75.766
1.75			
2.25	319	29	92.176
2.75			
3.25	325	31	95.625
3.75			
4.25	465	43	92.117
4.75			
5.25	257	28	107.368
5.75			
6.25	820	80	97.159
7.25			
8.25	1115	110	98.566
9.25			
10.25	1208	169	139.796
11.25			
12.25	597	60	101.311
13.25			
14.25	1334	148	111.216
15.25			
16.25	1158	124	107.057
17.25			
18.25	391	45	113.908
19.25			
20.25	566	50	87.628

Table B.7: Mercury analyses for sediment profiles for lake 36a.

Depth (cm)	Focus corr sed rate(g m^{-2} y^{-1})	Hg Sed Rate (µg$m^{-2}y^{-1}$)	Hg (ngg^{-1} DW)
0.25	316	97	307.74
1.25	118	32	273.51
2.25	160	34	214.83
3.25	146	26	176.05
4.25	215	36	165.53
5.25	292	42	142.36
6.25	2222	302	135.89
8.25	3081	328	106.43
10.25	269	31	116.07
12.25			116.17
14.25			104.81
16.25			126.12
18.25			130.56
20.25			125.90

Table B.8: Mercury analyses for sediment profiles for lake 36b.

Depth (cm)	Focus corr sed rate(g m^{-2} y^{-1})	Hg Sed Rate (µg m^{-2} y^{-1})	Hg (ngg^{-1} DW)
0.25	273	24	87.79
1.25	123	11	90.38
2.25	62	5	88.68
3.25	33	3	82.95
4.25	155	11	68.93
5.25	1364	96	70.04
6.25	179	12	69.43
8.25	63	5	73.35
10.25			74.12
12.25			70.97
14.25			71.68
16.25			72.99
18.25			79.18
			102.98

Table B.9: Mercury analyses for surface sediments for our 14 study lakes.

Lake	Depth (cm)	Hg (ng g^{-1} DW)	MeHg Conc. (ng g^{-1} DW)
2a	0.25	182	
9a	0.25	265	1.489
14a	0.25	125	1.452
36a	0.25	308	1.327
5a	0.25	171	0.446
6a	0.25	257	0.27
7a	0.25	281	0.683
2b	0.25	121	
9b	0.25	120	0.739
14b	0.25	78	0.365
36b	0.25	88	0.279
5b	0.25	99	0.281
6b	0.25	91	0.227
7b	0.25	96	0.221

APPENDIX C

Inferred Chlorophyll *a* in Sediment profiles

Table C.1: Inferred Chlorophyll *a*in sediments for lakes 2a and 2b.

Depth (cm)	Chla (mg g-1 DW)	Depth (cm)	Chla (mg g-1 DW)
1.25	0.01	1.25	0.03
2.25	0.01	3.25	0.02
3.25	0.01	4.25	0.01
4.75	0.01	5.25	0.01
6.25	0.01	7.25	0.02
9.25	0.01	9.25	0.02
12.25	0.02	12.25	0.01
18.25	0.01	15.25	0.01
24.25	0.02	18.25	0.01
28.25	0.01	21.25	0.01
32.25	0.02	24.25	0.01
36.25	0.01	28.25	0.01
		32.25	0.01
		36.25	0.01
		38.75	0.01

Table C.2: Inferred Chlorophyll *a*in sediments for lakes5a and 5b.

Depth (cm)	Chla (mg g^{-1}DW)	Depth (cm)	Chla (mg g^{-1}DW)
2.25	0.008	0.200	0.001
3.25	0.006	1.200	0.003
4.25	0.005	2.200	0.003
5.25	0.007	3.200	0.003
7.25	0.006	4.200	0.003
9.25	0.004	5.200	0.003
12.25	0.004	7.200	0.004
15.25	0.005	9.200	0.004
18.25	0.005	12.200	0.003
21.25	0.004	15.000	0.003
24.25	0.006	18.200	0.004
28.25	0.007	21.200	0.004
32.25	0.007	24.200	0.004
36.25	0.005	28.200	0.003
40.25	0.007	32.200	0.003
45.25	0.007	35.000	0.003

Table C.3: Inferred Chlorophyll *a*in sediments for lakes 6a and 6b.

Depth (cm)	Chla (mg g^{-1} DW)	Depth (cm)	Chla (mg g^{-1} DW)
0.25	0.0436	0.2500	0.0452
1.25	0.0422	1.2500	0.0565
2.25	0.0404	2.2500	0.0627
3.25	0.0397	3.2500	0.0338
4.25	0.0410	4.2500	0.0199
6.25	0.0400	5.2500	0.0188
8.25	0.0339	6.2500	0.0172
10.25	0.0208	8.2500	0.0171
12.25	0.0135	10.2500	0.0152
14.25	0.0113	12.2500	0.0162
16.25	0.0076	14.2500	0.0162
18.25	0.0083	16.2500	0.0150
20.25	0.0063	18.2500	0.0170
25.25	0.0074		
30.25	0.0052		

Table C.4: Inferred Chlorophyll *a*in sediments for lakes7a and 7b.

Depth (cm)	Chla (mg g^{-1} DW)	Depth (cm)	Chla (mg g^{-1} DW)
0.25	0.03420	0.20	0.00831
1.25	0.03029	1.20	0.00004
2.25	0.02767	2.20	0.00707
3.25	0.02519	3.20	0.00775
4.25	0.02173	4.20	0.00782
5.25	0.02157	5.20	0.00784
6.25	0.02131	7.20	0.00631
8.25	0.02198	9.20	0.00693
10.25	0.02449	12.20	0.00795
12.25	0.02893	15.00	0.00678
14.25	0.02747	18.20	0.00781
16.25	0.04088	21.00	0.01000
18.25	0.03751		

Table C.5: Inferred Chlorophyll *a*in sediments for lakes 9a and 9b.

Depth (cm)	Chla (mg g^{-1} DW)	Depth (cm)	Chla (mg g^{-1} DW)
0.25	0.051	0.250	0.039
1.25	0.048	1.250	0.039
2.25	0.045	2.250	0.040
3.25	0.041	3.250	0.046
4.25	0.039	4.250	0.046
5.25	0.035	5.250	0.038
6.25	0.032	6.250	0.031
8.25	0.029	8.250	0.020
10.25	0.023	10.250	0.024
12.25	0.022	12.250	0.019
14.25	0.021	14.250	0.022
15.75	0.022	16.250	0.017
		18.250	0.012
		20.250	0.009
		24.250	0.007

Table C.6: Inferred Chlorophyll *a*in sediments for lakes14a and 14b.

Depth (cm)	Chla (mg g^{-1} DW)	Depth (cm)	Chla (mg g^{-1} DW)
1.25	0.0483	0.25	0.0003
2.25	0.0485	1.25	0.0008
3.25	0.0441	2.25	0.0008
4.25	0.0387	3.25	0.0040
5.25	0.0392	4.25	0.0016
6.25	0.0386	5.25	0.0036
8.25	0.0321	6.25	0.0025
10.25	0.0285	8.25	0.0014
12.25	0.0266	10.25	0.0000
14.25	0.0263	12.25	0.0017
16.25	0.0266	14.25	0.0006
18.25	0.0270	16.25	0.0002
20.25	0.0273	18.25	0.0012
25.25	0.0333	20.25	0.0027
30.25	0.0333	25.25	0.0041
35.25	0.0281	28.75	0.0018

Table C.7: Inferred Chlorophyll *a* in sediments for lakes 36a and 36b.

Depth (cm)	Chla (mg g^{-1} DW)	Depth (cm)	Chla (mg g^{-1} DW)
1.25	0.03930	0.25	0.00036
2.25	0.03850	1.25	0.00512
3.25	0.02650	2.25	0.00815
4.25	0.02290	3.25	0.00731
5.25	0.02090	4.25	0.00089
6.25	0.02080	5.25	0.00075
8.25	0.01840	6.25	0.00100
10.25	0.02680	8.25	0.00079
12.25	0.02060	10.25	0.00084
14.25	0.02010	12.25	0.00106
16.25	0.02050	14.25	0.00086
18.25	0.02430	16.25	0.00087
20.25	0.02100	18.25	0.00186
25.25	0.02040	20.25	0.00774
30.25	0.02580	25.25	0.00425